Katholieke Universiteit Nijmegen

Project in High Energy Cosmic Rays

Air Shower Simulations for NAHSA

Author: Susana Cristina Cabral de Barros
Coordenator: Dr. Charles Timmermans

12th January 2003

Licenciatura em Física/Matemática Aplicada - Astronomia

Contents

Chapter 1

Introduction

Cosmic Rays are highly energetic particles that move through the universe. For charged particles, almost all the directional information is lost due to their interaction with magnetic fields. Probable sources for cosmic rays are supernovae, stellar winds, pulsars …

Cosmic rays are of great cosmological and astrophysical importance. For that reason, there are many experiments trying to measure cosmic rays spectrum, composition and origin.

High energetic cosmic rays, with energies above $3*10^{15}$ eV, can only be studied by their interaction with the atmosphere – causing extensive air showers. When a high energetic cosmic particle enters the earth' atmosphere it hits an air nucleus and creates secondary particles. These particles still have high energy, and will continue to fall through the atmosphere decaying or interacting with other nuclei. Each of them will create more particles originating a cascade.

The NAHSA experiment will measure the number of particles crated in the shower, which reach ground level, and use this number to reconstruct the energy of the primary particle.

Some of the experiments, which measure the cosmic ray energy spectrum, reported the existence of cosmic ray particles with energies of $3*10^{20}$ eV, which theoretically could not exist.

The energy measurement of this kind of experiments cannot be calibrated, the interpretation of the measurements is achieved by comparing experimental data with results of simulations. Therefore, we used air shower simulation packages to obtain a relation between the energy of the primary and its atomic number, and the density of the particles at ground level. Hence, the results depend on the model assumptions and on the quality of the simulation.

We used two existent air shower simulation packages: AIRES (AIR shower Extended Simulations) and CORSIKA (COsmic Ray SImulations for KAscade). Due to their complexity it is difficult to explain each of the approximations that were made for the interaction models. This makes it difficult to compare the results from different simulation packages. We chose to compare their results.

The programs consist of fully 4-dimensional Monte Carlo simulations of the particle transport and interaction through the atmosphere.

Chapter 2

Theory

2.1 Electromagnetic component:

2.1.1 Longitudinal development - The Heitler Model

Probably the simplest model that describes the development of an air shower is the Heitler model.

This model assumes that a particle will interact after a constant path length, creating two new particles. The energy is equally divided between the secondaries, each of them will undergo the same process until the particles reach a critical energy E_C. At this point the number of particles is maximum. After this maximum due to the number of particles only decreases.

Consequences of the Heitler model are that an air shower builds up, and gets re-absorbed into the atmosphere. At the shower maximum the following holds:

$$N(X_{\max}) = E_0 / E_C \qquad 1.1$$

Thus, all energy above a critical energy is used to create new particles. The depth in the atmosphere where this happens is given by:

$$X_{\max} = \lambda \frac{\ln(E_0 / E_C)}{\ln 2} \qquad 1.2$$

The formulae listed above are only valid for proton primaries. For nuclei, the primary energy E_0 is supposed to be shared between the (A) nucleons, thus changing formula 1.2 into:

$$X_{\max} \propto \lambda \ln(E_0 / (A.E_C)) \qquad 1.2b$$

In these formulae λ is the collision length.

The results listed above give a qualitative approximation of air shower development. A quantitative description is given by simulation packages CORSIKA and AIRES.

2.1.2 The sea-level distribution - NKG Formula

An alternative to Monte Carlo simulation is the Nishimura-Kamata-Greisen formula, that allows to calculate the number of particles at a given observation level. This formula reduces considerably the computation time but is less accurate.

The number of particles at sea-level gives an estimate of the total energy in the air shower. From the NKG formula or the AGASA experiment, we know that the total number of particles (or shower size) at ground level depends linearly on the total energy in the shower.

2.2 Muonic component:

2.2.1 Number of high energy muons

The number of high energetic muons (E_μ >>115 GeV) in a shower depends both on the primary energy, and on the chemical composition of the primary. When assuming the superposition principle, this relation is given by Elbert's formula:

$$\left\langle N_\mu \right\rangle \approx A \times \frac{0.0145 TeV}{E_\mu \cos\theta} \left(\frac{E_0}{A.E_\mu} \right)^{0.757} \left(1 - \frac{A.E_\mu}{E_0} \right)^{5.25} \qquad 2.1$$

When the energy of the primary particle is low, a shower initiated by a proton will produce less muons then a shower initiated by a heavy nuclei, because of the threshold factor.

At high energy $E_0 >> AE_\mu$ we can see that there is not much difference in the number of muons, in a shower initiated by a proton and a shower initiated by a heavy nuclei. In fact, this relationship goes like:

$$N_\mu (> E_\mu) \propto A^{0.243} \qquad 2.1b$$

Therefore, it is difficult to distinguish the composition based in muons rates.

The theory also calculates muons with energy above 1 GeV because those can pass trough the concrete used experimentally to separate the electromagnetic part of the shower and the muonic part.

We used a cut-off of 1 GeV for muons to compare the data obtain in the Monte Carlo simulations with the theory.

Assuming one muon per pion, and the Feynman-scaling being valid we can estimate the total number of muons with energies above 1 GeV, in a shower initiated by a nucleon, which is given by:

$$N_\mu (> 1GeV) = AB\left(\frac{E_0}{A\varepsilon_\pi}\right)^{p_\mu} \qquad 2.2$$

In here A is the mass number of the primary, p_μ and B are model dependent constants. Using the code by Elbert the results are in accordance with 2.2 with B = 2.8 and p_μ = 0.86.

2.2.2 The importance of the muonic component

When the primary particle is hadronic, the development of the shower is very different and more complex than a simple electromagnetic cascade. An analysis of the electromagnetic component alone is not enough to distinguish between the two types.

Although the muonic component is much smaller than the electromagnetic, the study of the muonic component is

important because:

- As NAHSA samples at a single depth, it isn't possible to measure the energy of the primary particle without a model-dependence for electromagnetic particles.

- Muons only loose little energy by ionisation so the number of muons doesn't decrease as much as the number of electrons after reaching the maximum.

- At a fixed level the number of muons in a shower initiated by proton is bigger then the number of muons in a shower initiated by an iron nucleus with the same total energy. Therefore it may help to determine the composition of the primary particle.

In order to obtain a relation between shower size and primary energy, simulation programs are used. However, fluctuations in number of particles for fixed E_0 and the model dependency of the shower development made this a complicated problem.

Chapter 3

Simulation Programs

3.1 Theory

The distance a particle travels before it undergoes its next inelastic interaction or decay is determined by the cross section for a hadronic reaction together with the atmospheric density distribution along the flight path, and the probability to decay.

Although stable particles only interact, for the unstable particles there exists a competition between the two processes. The actual path-length is determined by both the decay-length and the interaction-length.

While the theory of the electromagnetic and weak interaction is quite well understood, the hadronic interaction models have problems because they have to be extrapolated using theoretical models to calculate cross sections in the forward direction at high energies.

3.2 Interaction Models

3.2.1 Hadronic shower

Hadronic interactions are simulated by several external models, depending on energy. If the energy is high enough, the interaction is treated alternatively with one of the models VENUS, QGSJET, DPMJET, SIBYLL, or HDPM.

When the energy is lower then 80 GeV normally GHEISHA is used.

The first hadronic models were phenomenological; they consisted of parameterisations of the accelerator results, which were extrapolated to high energies. One of the assumptions is the superposition model, where the nucleus is assumed to be just a superposition of free nucleons.

Lately microscopic models were developed based on more theoretical foundations. They use the Gribov-Regge Theory (GRT) to simulate interactions of nucleons and nuclei. QGSJET, VENUS, DPMJET and neXus are GRT high energy models

for cosmic rays.

SIBYLL is a high energy model between phenomenological and GRT, it's a mini jet model inspired in QCD. SIBYLL was recently revised and agrees with experimental results much better then before.

GHEISHA is a phenomenological model and the one more often used to low energy hadronic interactions.

In AIRES and CORSIKA when the energy is above a threshold the hadronic inelastic collisions and photonuclear reactions are calculated with external interaction models (like SIBYLL and QGSJET), otherwise they are calculated using an extension of Hillas' splitting algorithm, which is a simpler and much faster model.

In the Hillas splitting algorithm the initial energy is split at random into smaller and smaller portions. The secondary particles are created from these energy packets, assigning their identity according to externally provided probabilities.

3.2.2 Electromagnetic shower

The electromagnetic interactions are well described by QED and can be accurately simulated using, for example, EGS4. In CORSIKA and AIRES electron and photon reactions are treated with EGS4 or with the analytic NKG formula.

- EGS4 gives detailed information (momentum, space coordinates, propagation time) of all electromagnetic particles, but needs extensive computing times, which increases linearly with the primary energy.
- In the NKG option the electromagnetic component is calculated by an analytic approach without a full Monte Carlo simulation, which is faster than EGS4, but only gives electron densities at selected points in the detection plane.

3.3 Simulation Parameters

In the simulation programs studied, initially several parameters have to be set, such as:

- Primary energy
- Primary angle of incidence
- Energy cut-off, specified for hadrons, muons,

electrons and photons, separately
- Interaction models
- Thinning sampling option
- Atmospheric model
- Magnetic field strength and direction

The random numbers are adequately generated by means of a built-in pseudorandom number generator.

3.3.1 Thinning algorithm

In order to decrease the computation, simulations use a statistical sampling mechanism thus only propagating a representative fraction of the total number of particles, which is appropriately weighted.

Thinning is invoked whenever new particles are generated. If the sum of the energies of all secondaries is below the thinning energy, only one of the secondaries is followed, selected randomly conform its energy and is given an appropriate weight. Due to this impartial sampling, average values calculated with the weighted particles do not depend on the thinning energy. However, thinning introduces additional statistical fluctuations that depend on the thinning energy.

CORSIKA uses the original statistical thinning algorithm introduced by A. M. Hillas while AIRES uses its own version of it. In which, if the statistical weight of a particle is beyond a specified value, it’s no longer thinned and more particles continue to be propagated instead of just one with a bigger statistical weight. This increases computing time but significantly reduces the thinning fluctuations. Thinning energy and weight limit can be optimised to reduce fluctuation using a minimal computing time.

3.3.2 Atmospheric model

The new versions of AIRES and CORSIKA take into account the earth’ curvature, if the corrections are important. Near the shower axis, they use the approximation of a plane earth. The distance to the shower axis where the

approximation is valid was carefully calculated, and increases with the altitude.

The atmospheric model used is the US standard with the density parameterized by Linsley; the atmosphere consists of 5 spherical shells with four transition zones. The composition of the atmosphere consists of particles with a mean molecular weight based upon a mixture of N, O and Ar and other elements in the right amounts.

3.3.3 Magnetic Field

The direction and strength of the magnetic field is important because it deflects charged particles. In our case it was calculated automatically using International Geomagnetic Reference Field (IGRF) in the case of AIRES and Geomag in the case of CORSIKA; using the altitude and geographic coordinates of Nijmegen as well as the date of the event.

3.4 The physics of CORSIKA and AIRES

A recent paper from J. Knapp, D. Heck, S.J. Sciutto, M.T. Dova and M. Risse compares the hadronic models QGSJET and SIBYLL. They stated that the differences have decreased in the newest versions. But they still affect the longitudinal development of shower and consequently the particle number at ground level and their lateral distribution, the height of the maximum of the shower and the total energy of the electromagnetic component. They conclude that differences in longitudinal development and lateral distribution of the shower are bigger at higher energies. They also conclude that the superposition assumption is not accurate.

AIRES can be more than 3 times faster then CORSIKA and its output is smaller, due to a different compression algorithm.

The longitudinal development agrees within 3%. For the lateral distribution, at large distances to the core there are differences between the two programs but near the core they agree very well.

3.4.1 AIRES

The physical algorithms of AIRES are the modern equivalent to MOCCA code created by A. M. Hillas, and the other existent shower simulation programs were also study to create AIRES.

The main characteristics of AIRES simulation program are:

Propagated particles	Gammas. Leptons: $e^{\pm}$, $\mu^{\pm}$. Mesons: π^0, $\pi^{\pm}$; η, $K^0_{L,S}$, $K^{\pm}$. Baryons: p, $\bar{p}$, n, $\bar{n}$, Λ. Nuclei up to $Z = 26$. Neutrinos are generated (in decays) and accounted for their number and energy, but not propagated.
Primary particles	All propagated particles can be injected as primary particles. Multiple and/or "exotic" primaries can be injected using the *special primary* feature.
Primary energy range	From 800 MeV to 1 ZeV (10^{21} eV).
Geometry and environment	Incidence angles from vertical to horizontal showers. The Earth's curvature is taken into account for all inclinations. Realistic atmosphere (Linsley model). Geomagnetic deflections: The geomagnetic field can be calculated using the IGRF model [8].
Propagation (general)	Medium energy losses (ionization). Scattering of all charged particles including corrections for finite nuclear size. Geomagnetic deflections.
Propagation: *Electrons and gammas*	Compton and photoelectric effects. Bremsstrahlung and e^+e^- pair production. Emission of knock-on electrons. Positron annihilation. LPM effect, and dielectric suppression. Photonuclear reactions.
Propagation: *Muons*	Bremsstrahlung and muonic pair production. Emission of knock-on electrons. Decay.
Propagation: *Hadrons and nuclei*	Hadronic collisions using the EHSA (low energy) and QGSJET or SIBYLL (high energy). Nuleus-nucleus collisions via QGSJET or SIBYLL, or using a built-in nuclear fragmentation algorithm. Hadronic cross sections are evaluated from fits to experimental data (low energy), or to QGSJET or SIBYLL predictions (high energy). Emission of knock-on electrons. Decay of unstable hadrons.
Statistical sampling	Particles are sampled by means of the Hillas thinning algorithm [4], extended to allow control of maximum weights.
Main observables	Longitudinal development of all particles recorded in up to 510 observing levels. Energy deposited in the atmosphere. Lateral, energy and time distributions at ground level. Detailed list of particles reaching ground, and/or crossing predetermined observing levels.

Adapted from "AIRES: A system for air shower simulations"

3.4.2 CORSIKA

Three programs (ISOBAR hadronic interaction model low energy, HDPM high energy, EGS4 electromagnetic part of shower) were merged together to form CORSIKA.

The main characteristics of the CORSIKA simulation program are:

Propagated particles	Gammas. Leptons: $e^{\pm}, \mu^{\pm}$ Mesons: $\pi^0, \pi^{\pm}; \eta, K^0_{L,S}, K^{\pm}$. Baryons: $p, \overline{p}, n, \overline{n}, \Lambda$. Strange Baryons $\Xi^{\pm}, \Xi^0; \Sigma^{\pm}, \Sigma^0; \Omega^{\pm}; \omega; \rho^{\pm}, \rho^0$ Nuclei up to A=59 Neutrinos are generated (in decays) and accounted for their number and energy, but not propagated.
Primary particles	All propagated particles can be injected as primary particles. Or "mixtures" of particles
Primary energy range	From 80 GeV to 1018 eV
Geometry and environment	Incidence angles from vertical to horizontal showers. The Earth's curvature is taken into account for big inclination angles. Realistic atmosphere: USA atmosphere (Linsley model) and Europe and South Pole atmospheric models for various seasonal days. Geomagnetic deflections: The geomagnetic field can be specified or calculated using Geomag
Propagation (general)	Medium energy losses (ionization). Scattering of all charged particles including corrections for finite nuclear size. Geomagnetic deflections for all charged particles
Propagation: Electrons and gammas	Compton and photoelectric effects. Bremsstrahlung and e+/e- pair production. Emission of knock-on electrons. Positron annihilation. LPM effect and dielectric suppression. Photonuclear reactions. Electromagnetic interactions: NKG and EGS4
Propagation: Muons	Bremsstrahlung and muonic pair production. Decay. Deflection by multiple coulomb scattering

Propagation: Hadrons and nuclei	External hadronic interaction models available: VENUS, QGSJET, DPMJET, SIBYLL, HDPM, URQMD and GHEISHA Emission of knock-on electrons. Decay of unstable hadrons.
Statistical Sampling	Particles are sampled with the Hillas thinning algorithm.
Main Observables	Detailed list of particles reaching ground, and/or crossing predetermined observing levels. Longitudinal development of the shower Energy deposit in the atmosphere Time of fight Cherenkov Radiation

For more information about CORSIKA or AIRES please consult the respective manuals.

Chapter 4

Longitudinal Distribution

4.1 Procedure

In order to compare CORSIKA and AIRES with the theoretical description of shower development, we used the longitudinal development of the shower, because there are simple intuitive theoretical models, as outlined in chapter 2.

For CORSIKA, an input file, similar as the one shown in appendix A.1, was used. Showers were simulated, varying in primary energy between 10^{13} eV and 10^{14} eV (larger was impossible with PLOTSH option). The primary particle was either proton or iron. The atmosphere was chosen to be European or USA standard. We use the PLOTSH option to obtain three files containing the energy, start and ending positions of all particles subdivided into electromagnetic, muonic and hadronic.

An AIRES input file is shown in appendix A.2. The program was ran for one additional energy, namely 10^{15} eV, and only for USA standard atmosphere. Special care was taken in order to assure that other variables were chosen similar to the ones that were used in CORSIKA, like the magnetic field, cut off energies, etc.

In CORSIKA the notation used was the following:

	Proton		Iron	
Europe	INPUTD*	runnr = 0*	INPUTF*	runnr = 1*
USA	INPUTG*	runnr = 2*	INPUTH*	runnr = 3*

* = 3, 4 and represents and energy of 10^{1*} eV.

With PLOTSH version these are the highest energies possible. For higher energies the tracks.em file is bigger than allowed by the computer system.

The runnr is an input option and is used on the output files tracks**runnr**.em, tracks**runnr**.had and tracks**runnr**.mu respectively for electromagnetic component, hadronic component and muonic component.

The interaction model for hadrons used was SIBYLL 2.1 in both AIRES and CORSIKA.

The atmospheric model can be chosen by the option ATMOD, where 1 is the USA standard, and 5 was the one that was used for Europe (though more options exist). The USA standard is a more refined model, where special caution was taken to have smooth transition between adjacent atmospheric layers.

Analysing simulations with different thinning we conclude that the thinning affects the number of particles obtained in the tracks files. This means that the results presented in these files aren't automatically corrected for thinning and to obtain reliable results it is important to put it inactive.

The cut-off energies used in both CORSIKA and AIRES were:

Gamma - 3.0 MeV
Electron - 3.0 MeV
Muon - 1.0 GeV
Nucleons - 300 MeV

For CORSIKA, we used a cut-off energy of 300 MeV for muons during simulation. Only in the analysis a cut-off of 1 GeV was used.

The treatment of CORSIKA data consists of reading the output file and use the start- and end-position of each particle track to count the number of particles within 50 m high atmospheric layers. This results in 400 bins from 0.0 m to 20 km altitude. Afterwards, the number of particles versus the altitude (in cm) was plotted. The routine used to count the number of particles is given in appendix B.1.

For Aires the following notation is used:

	Proton	Iron
Input	INPUT0*	INPUT1*
Task	Proton0*.extension	Iron1*.extension

* =3, 4, 5 and represents an energy of 10^{1*} eV.

It was possible to go to higher energies but the ones listed above were used in order to be able to compare the results with CORSIKA.

Aires has an option to export tables with the number of particles of a given type that pass through a layer in the atmosphere. It's possible to choose the number of layers as

well as the start and the ending position of the binning. We chose to use 400 bins. The altitude is given in atmospheric depth (g/cm^2) and the parameterization of the atmospheric model was used to create a routine that converts atmospheric depth into altitude. This routine is given in appendix B.2. After the conversion of the atmospheric depth to altitude the tables were used to plot the number of particles versus the altitude in metres.

In Aires we can choose an output table where the particle weight is taken into account, so it corrects for thinning. Therefore, a thinning of 10^{-4} was used, thus shortening the CPU time considerably.

The tables used were:
t1001 - gamma
t1205 - electrons and positrons
t1207 - muons
t1022 - protons
t1211 - pions

The results of t1001 and t1205 were added to obtain the electromagnetic component of the air shower and compare it with CORSIKA. The numbers of protons and pions are very small so the fluctuations are very important. Besides, there are no simple theoretical models thus the behaviour of protons and pions wasn't analysed and the numbers are not given in the tables, although they are plotted along with the other components.

Next to the code for counting the number of particles in CORSIKA and transforming atmospheric depth in altitude in AIRES, additional software was written to read the files, and create plots. The PAW-package was used for final plotting.

In CORSIKA the random numbers were specified but in AIRES they were arbitrary.

When the plots were smooth, a program was used to read-off the number of particles at ground level and at the maximum position and the altitude of the maximum. In all the other cases this amounts were estimated by eye.

4.2 Results

4.2.1 CORSIKA - Number of particles obtained

Muons		**10^{13} eV**	**10^{14} eV**
Proton	Z=0	130	1 373
	Nmax	177	1 409
	Z(Nmax)m	5 150	40
Iron	Z=0	302	1 854
	Nmax	467	2 438
	Z(Nmax)m	6 500	6 900
EM		**10^{13} eV**	**10^{14} eV**
Proton	Z=0	1 033	74 629
	Nmax	23 500	397 727
	Z(Nmax)m	9 500	5 300
Iron	Z=0	1 419	6 903
	Nmax	22 069	261 811
	Z(Nmax)m	8 500	8 100

Table 1: USA standard atmosphere

Muons		**10^{13} EV**	**10^{14} eV**
Proton	Z=0	137	779
	Nmax	200	981
	Z(Nmax)m	5 150	5 250
Iron	Z=0	352	1 926
	Nmax	580	2 394
	Z(Nmax)m	8 400	6 050
EM		**10^{13} eV**	**10^{14} eV**
Proton	Z=0	1 290	17 531
	Nmax	32 683	387 763
	Z(Nmax)m	5 500	6 650
Iron	Z=0	381	15 630
	Nmax	19 767	241 467
	Z(Nmax)m	8 500	8 300

Table 2: European atmosphere

4.2.2 AIRES - Number of particles obtained

MUONS		**10^{13} eV**	**10^{14} eV**	**10^{15} eV**
Proton	Z=0	85	725	6 541
	Nmax	120	860	6 800
	Z(Nmax)m	6 100	5 600	2 400
Iron	Z=0	234	1 494	11 000
	Nmax	995	1 900	13 600
	Z(Nmax)m	8 000	6 500	4 000
EM		**10^{13} eV**	**10^{14} eV**	**10^{15} eV**
Proton	Z=0	2 129	34 600	392 700
	Nmax	34 000	260 000	2 850 000
	Z(Nmax)m	4 900	5 000 +/- 1500	6 000 +/- 2000
Iron	Z=0	806	7 561	200 861
	Nmax	19 500	198 500	2 300 000
	Z(Nmax)m	9 100	8 550 +/- 1500	6 000
GAMMA		**10^{13} eV**	**10^{14} eV**	**10^{15} eV**
Proton	Z=0	1 753	29 556	322 000
	Nmax	31 000	212 500	2 300 000
	Z(Nmax)m	4 750	5 000	6 000
Iron	Z=0	620	6582	159 000
	Nmax	16 000	156 000	1 900 000
	Z(Nmax)m	9 000	8 500	5 500
e^-/e^+		**10^{13} eV**	**10^{14} eV**	**10^{15} eV**
Proton	Z=0	376	5 044	70 700
	Nmax	7 600	518 000	565 000
	Z(Nmax)m	5 100	5 500	6 000
Iron	Z=0	186	979	41 861
	Nmax	3 900	41 800	468 000
	Z(Nmax)m	9 500	8 500	6 750

Table 3: USA standard atmosphere

In the above tables: Z = 0, is the number of particles at ground level, Nmax is the number of particles at maximum position and Z(Nmax) is the altitude of the maximum position.

The error on Z(Nmax) is about 1 km in most cases. Otherwise, the value is specified.

Plots were made, for each component of each shower for both CORSIKA and AIRES. Due to the number of plots involved, only the AIRES results are presented here, in figures 1 to 6.

4.3 Discussion of the Results

4.3.1 General Features

From the tables and graphics we can verify that:

1.1 - The quantitative analyses can only be applied to AIRES results because in the case of CORSIKA the numbers represent the quantity of particles in a bin of 50 m high and not the quantity that passes through a layer. But we can see that the qualitative description holds.

1.2 - The maximum number of particles is reached first for the hadrons (at higher altitude), afterwards for electromagnetic particles, and finally for muons. This fact can be easily understood theoretically because the shower is initiated by hadrons, first it creates more hadrons and then the electromagnetic shower. The muons are created by the decay of pions and kaons, and have a long live-time (or larger path-length than electrons).

1.3 - The most common type of particle is electromagnetic, although the difference is attenuated near the ground level due to the fact that the number of muons only decreases slightly after the maximum while the electromagnetic number decreases rapidly after the maximum due to ionization.

4.3.2 Electromagnetic Shower

2.1 - The number of particles at ground level and at maximum position is directly proportional to the energy of the primary particle. This fact is in agreement with equation

$$N\left(X_{\max}\right) = E_0 / A.E_C \qquad (1.1)$$

There is only one exception in AIRES for Iron the

ratio between the number of particles at ground level for energy 10^{15} and 10^{14} is 26.6 instead of 10. In this particular case, we can also acknowledge that the two components of the electromagnetic shower (e^-/e^+ and gamma) have deviations of the expected value and for the e^-/e^+ the difference is bigger (42.7) than for the gamma (24.15), but the majority of electromagnetic particles are gamma.

2.2 - As it was expected, for all components of the shower, if the primary particle is an iron nucleus there are less electromagnetic particles at ground level and at the maximum compared to proton induced showers. At maximum the ratios are in agreement with equation 1.1. This happens because the energy of the primary is divided between the 56 nucleons.

2.3 - The bigger the energy of the primary particle the lower is the altitude of the shower maximum. That was also the result obtain with the Heitler model:

$$X_{\max} \propto \lambda \ln\left(E_0/(A.E_C)\right) \qquad (1.2b)$$

2.4 - The ratio between a shower generated by a proton and one generated by an iron nucleus can also be explained by the same formula. In fact, based on the tables we can conclude that, the maximum of the shower is reached first (at higher altitude) if the particle is an iron nucleus.

4.3.3 Muonic Shower

3.1 - The number of particles at ground level and at maximum position is roughly proportional to the energy of the primary particle, in accordance with equation:

$$N_\mu\left(>1GeV\right) = AB\left(\frac{E_0}{A\varepsilon_\pi}\right)^{0.86} \qquad (4.1)$$

That means that when the energy increases by a factor of 10 the number of particles should increase by a factor of 7.2 approximately. Our results are in agreement with that.

3.2 - If the primary particle is an iron nucleus (A=56) there are more muons at ground level then when the particle is a proton.

We have two formulas for the number of muons at ground level:

$N_\mu(>1GeV) \propto A^{0.14}$ from (4.1) → N(Fe) = 1.76N(p).

$N_\mu(>E_\mu) \propto A^{0.243}$ from (2.1b) → N(Fe) = 2.65N(p).

Our results are consistent with a power of A between 0.14 and 2.65. The behaviour at maximum position can be satisfactorily explained by the same formulas.

3.3 - The bigger the energy of the primary particle the lower the altitude of the shower maximum, as was expected theoretically. This happens because a particle with a bigger energy interacts sooner with the atmosphere.

4.3.4 Comparison between CORSIKA and AIRES

It's possible to verify that the results of CORSIKA and AIRES agree with each other.

Normally the number of particles in CORSIKA is bigger than the number of particles obtain using AIRES but that can easily be understood when we take into account that the two numbers do not represent exactly the same thing, as was explained before. The two cases where AIRES results are bigger then CORSIKA, can be explained by fluctuations in the shower generation.

The position of the maximum depends on the altitude of the first interaction, which is random, and therefore different in each simulation. This affects the number of particles produced in a shower randomly. We could choose the altitude of the first interaction in the simulation and control the fluctuations of particles due to that, but that was not done.

4.3.5 Comparison between CORSIKA USA Atmosphere and Middle Europe Atmosphere

The values obtained for both atmospheres are in reasonable agreement with each other. Of course, there are some fluctuations due to the randomness of the event.

In the USA Atmosphere, the position of the maximum for primary energy of the proton of 10^{14} eV is quit strange. From a more detailed analysis of the plot, we conclude that this behaviour isn't normal. We can see that the number of particles was constant and then starts to increase again after the layer at an altitude of 4 km, which is a transition point. This behaviour is not expected. None of the other plots show this behaviour.

Chapter 5

Lateral Distribution

5.1 Procedure

In order to obtain the lateral distribution in AIRES, we have to change some of the input parameters:

Task
Ground Altitude 45 m
Primary Zenith Angle
Gamma/Electron/Muon/Nucleon cut-off Energy 10 MeV
Thinning
TotalShowers

Export tables:
T2001 – gamma lateral distribution
T2205 – electrons and positrons lateral distribution
T2207 – muons lateral distribution
T2291 – charged particles lateral distribution

Basically all we have to do is change the exported tables. This means that we can obtain all the information needed (for the longitudinal development and the lateral distribution) running the program just one time, with the appropriate exported tables. The other changes were improvements. (which we learned from experience with previous simulations)

The density of particles per square meter vs. the distance to the shower-core, is given in the exported tables where we used 40 bins from 50 m up to 1823.81 m.

We have made simulations for 10 showers and a primary energy of 10^{15} eV, using thinning values of 10^{-4} and 10^{-6} to investigate the effect of thinning in the output tables. Using a thinning of 10^{-4} the program runs in two minutes, but fluctuations were big. With 10^{-6} thinning it took 1 hour but the fluctuations were much smaller, as it can be seen in the next plot.

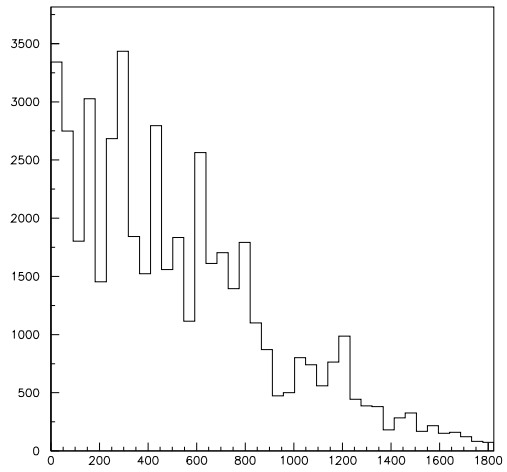

thinning of 10^{-4} relative

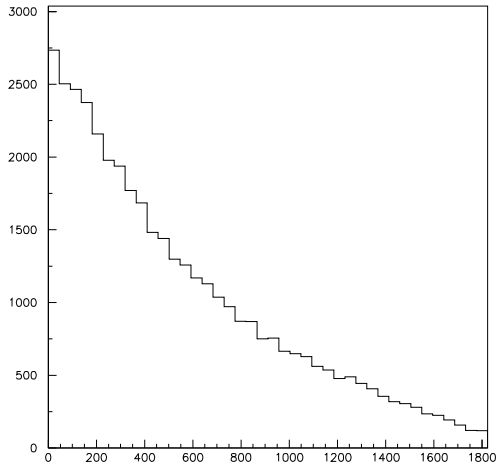

thinning of 10^{-6} relative

Simulations with 10 and 100 showers were performed to compare the results.

For the creation of 100 showers the computation time is around 10 hours at an energy of 10^{15} eV and 31 hours for a shower energy of 10^{17} eV. These times are acceptable for the purpose of this project.

Therefore we chose a thinning of 10^{-6} as a compromise between small fluctuations and acceptable computation times.

For vertical showers, the following notation was used:

	Proton	Iron
Input	INPUTP#*	INPUTI#*
Task	P#*.extension	I#*.extension

= A for 10 showers and B for 100 showers
* = 15, 16, 17 and represents and energy of 10^{*} eV.

For inclined showers the notation was:

	Proton	Iron
Input	INPUTPB§*	INPUTIB§*
Task	PB§*.extension	IB§*.extension

§ = 1, 2, 3, 4 respectably for inclined showers with 10, 20, 30, 40 degrees

The program was ran for three energies 10^{15}, 10^{16} and 10^{17} eV, and for various inclinations angles 0º, 10º, 20º, 30º and 40º, in order to investigate the dependence of the particle density at ground level to the primary energy and to the inclination of the shower axis.

I used PAW to plot the results directly. The plots were made both in linear and in logarithmic Y-scale, which provides a better insight into the results. Plots were made to compare various characteristics: the energy dependence, the inclination angle dependence, the difference between proton and iron initiated showers and the relative behaviour of the different particles.

Also the AGASA function was plotted for the charged particles, however it does not fit the results. The AGASA function and the plot routine are given in appendix B.3.

5.2 Vertical showers

5.2.1 Results

We have made a comparison of the results obtain for 10 and 100 showers for proton and iron primaries. Figures 7 to 14 contain lateral distributions for primary energies of 10^{15} eV and 10^{17} eV. A primary energy of 10^{16} eV has also been studied.

The number of particles near the shower core is presented in the next table:

Charged		**Dist core m**	**10^{15} eV**	**10^{16} eV**	**10^{17} eV**
10	Proton	[0,50]	8.417	202.641	2029.40
		[50m,55]	1.450	27.448	282.072
	Iron	[0,50]	2.301	61.787	1052.87
		[50m,55]	0.605	11.412	180.569
100	Proton	[0,50]	10.602	145.869	2286.03
		[50m,55]	1.728	21.978	307.663
	Iron	[0,50]	2.550	58.555	1045.96
		[50m,55]	0.655	11.481	172.355
EM		**Dist core m**	**10^{15} eV**	**10^{16} eV**	**10^{17} eV**
10	Proton	[0,50]	8.270	201.024	2018.40
		[50m,55]	1.380	26.772	277.599
	Iron	[0,50]	2.139	60.187	1037.34
		[50m,55]	0.517	10.641	173.635
100	Proton	[0,50]	10.444	144.531	2274.67
		[50m,55]	1.656	21.340	302.908
	Iron	[0,50]	2.383	56.939	1030.92
		[50m,55]	0.564	10.688	165.485
GAMMAS		**Dist Core m**	**10^{15} eV**	**10^{16} eV**	**10^{17} eV**
10	Proton	[0,50]	25.398	587.796	5996.50
		[50m,55]	6.555	120.587	1266.67
	Iron	[0,50]	6.678	181.409	3171.42
		[50m,55]	2.242	48.634	762.589
100	Proton	[0,50]	31.550	436.396	6778.82
		[50m,55]	7.486	98.636	1409.79
	Iron	[0,50]	7.359	174.454	3139.07
		[50m,55]	2.342	46.873	756.165
MUONS		**Dist core m**	**10^{15} eV**	**10^{16} eV**	**10^{17} eV**
10	Proton	[0,50]	0.1183	1.194	8.165
		[50m,55]	0.06305	0.6098	3.936
	Iron	[0,50]	0.1476	1.365	12.352
		[50m,55]	0.08543	0.7194	6.367
100	Proton	[0,50]	0.1264	1.032	8.394
		[50m,55]	0.06584	0.5262	4.216
	Iron	[0,50]	0.1517	1.369	12.045
		[50m,55]	0.08646	0.7399	6.287

The plots of the distribution of particles at ground level and the tables presented show that there are no significant differences between 10 or 100 showers. In the plots, 100 showers seem to have generated more particles at ground level but that's just a random effect, in fact using a primary energy of 10^{16} eV showed the opposite, as it can

be seen in the tables.

Due to the fact that 100 showers have lower fluctuations, it's advisable to use it whenever the computation time is short enough. So from now on, the simulation of 100 showers is going to be used.

In the next tables the ratio of the number of particles for proton and iron induced showers is shown.

Electromagnetic - Longitudinal distribution

energy	10^{13} eV	10^{14} eV	10^{15} eV
Z=0	2.64	4.57	1.95
Z=max	1.74	1.32	1.29391

Electromagnetic - Lateral distribution

energy	10^{13} eV	10^{14} eV	10^{15} eV
Z<50	4.38	2.538	2.2064
50<55	2.936	1.9966	1.830

Muons - Lateral distribution

energy	10^{13} eV	10^{14} eV	10^{15} eV
Z<50	1.7023	1.3266	1.4349
50<55	1.31	1.406	1.4912

We have plotted the ground-level distributions of the different particles in the same plot to be able to compare their relative behaviour. The results are shown in figures 15 to 18.

Also, the AGASA function was fitted to the lateral distribution of charged particles as shown in figures 19 and 20.

5.2.2 Discussion of the Results

Near the core

The numbers confirm the linear dependence of the number of particles at sea level, with respect to the primary energy, near the core, which was already tested in the longitudinal study. The other formulae for the number of particles at ground level are also confirmed, in particular the ratio of particle numbers from proton and iron induced showers. The ratio N(p)/N(Fe) for gamma and electromagnetic part is a little bigger then log(56)= 1.7 the expected value. For the muonic part the results are consistent with $N(Fe) = A^k N(p)$ with k between 0.14 and 0.243, as was expected. For all charged particles, consisting of the sum of electromagnetic and muonic near the core, the behaviour is dominated by the electromagnetic part as there are much more electromagnetic particles then muons.

Distribution

From the plots showing the lateral development of a shower we can conclude that:

1. **General behaviour** - as was expected, the number of particles decreases almost exponentially with the distance to the core.

2. **Dependence in the energy of the primary** - the number of particles is directly proportional to the energy of the primary particle as was already concluded in section 4.3.2. Also plots were made, comparing the different energies at same time. From these we see that the shape of the particle density versus distance to the core is not exactly the same for all energies. It appears that when the energy is bigger the shower is relatively narrower.

3. **Dependence in the composition of the primary** - Especially the first plots are useful in comparing the differences in the density of particles between showers of different primaries:

   3.1 For gammas, charged particles and electrons and positrons, near the core, there are more particles if the primary particle is a proton. However, at larger distances there are more particles if the primary is an iron nucleus. This means that showers initiated by iron extend more then the ones initiated by protons.

   3.2 For muons there are always more particles if

the primary is an iron nucleus and the ratio between iron and proton initiated shower seems to be the same at all distances to the core.

4. **The different components of a shower** - Especially the last plots are useful for comparing the behaviour of the different types of particles:

4.1 The most common type is gamma and the least abundant are the muons up to a turning point. The charged particles are dominated by e^+/e^- at first, but after the turning point they are dominated by muons. This is due to the fact that the e^+/e^- decrease much faster with the distance then muons, that is the electromagnetic shower is narrower then the muon one.

4.2 The (muon, e^+/e^-) turning point depends on the energy: the bigger the energy, the farther from the core axis the turning point is located. It also depends on the composition of the primary: for proton initiated showers the turning point is farther from the core axis.

4.3 The density of gammas decreases more rapidly with distance to the core then the density of muons. But, because the number of gammas is much bigger then the number of muons the (muon, gamma) turning point can’t be seen in the plots, it probably occurs after the 1800 m of distance from the core.

As was expected the hadronic part of the shower is narrower then the electromagnetic part, and the muonic part spreads to even larger distances.

AGASA function

The AGASA function does not fit the results at any energy studied, neither for proton nor for iron initiated showers.

It's not just a mere shift in the x or y-axis, the shape of the AGASA function is different from the distribution of charged particles.

5.3 Inclined Showers

We ran AIRES for various inclinations, in order to investigate the dependence of the ground level distribution on the inclination angle. The result obtained is the distribution of particles in a plane perpendicular to the shower axis, which has to be projected onto the ground level.

This is not only a factor of the cosine of the inclination angle, as we have to take into account that some particles have to cross more atmosphere, thus arrive later at the ground which means a larger spread, thus the shape of the plots is oval and not just elliptical.
A program from S. J. Sciutto exists for this purpose, but I unfortunately did not have access to it.

5.3.1 Results

The lateral developments of the four components of showers with different inclination angles (0º, 10º, 20º, 30º and 40º), primary energies (E_0 = 10^{15} and 10^{17} eV) and primary particles (proton and iron), are plotted in figures 21 to 36.

Figures 37 to 40 show the relative behaviour of the various particles for showers with an inclination angle of 40º.

5.3.2 Discussion of the Results

From the plots of the lateral distribution of all types of particles at different inclination angles and the comparison between the plots of the ground distribution at 0º and 40º we can conclude that:

1. In an inclined shower the distance that the particles have to travel in the atmosphere is bigger, or in other words, the shower axis is bigger. So, the larger the inclination angles the more extensive is the shower, and therefore, near the core the bigger the inclination the lower the density of particles.

2.This dependence is not linear: the difference between 0º and 20º is much smaller than between 20º and 40º. This is geometrically intuitive because the size of the shower axis does not depend linearly of the inclination angle.

3.This difference seems to be even bigger when the energy of the primary is higher. The turning point (where the density of particles in a shower with inclination angle = 20º becomes bigger then in a 40º one) is nearer the shower axis for a higher primary energy.

4.As already stated, the shape of the dependence of the density of particles depends on the inclination angle but it also depends on the component that is being analysed. This can easily be seen in the logarithmic plots. The e^+/e^- have a nearly exponential decay while muons and gamma do not. The charged component is dominated by the e^+/e^-, therefore it also has a nearly exponential decay.

5.The electromagnetic component of the shower is narrower then the muonic part, as in vertical showers.

Chapter 6

Conclusions

6.1 Longitudinal distribution

All the features of air showers that were analysed are in agreement with the theoretical models. Qualitatively all these aspects are understood.

The two simulation programs agree within fluctuations, which are relatively large due to a single shower simulation, which could be non-typical.

6.2 Lateral distribution

The purpose of this project was to determine a relation between the density of particles at ground level and the primary energy and composition of a given air shower.

We obtained some clues, which may help obtaining such a relation.

The problem in obtaining the primary energy given the lateral distribution in first approximation is due to two major unknowns about the primary: its composition and its energy.

The inclination angle can be calculated by the shape of the lateral distribution and delay times.

After knowing the inclination angle the composition could be obtained using the ratio of muons/e+e-, but that is not possible within NAHSA.

If we manage to know the composition and direction, the energy of the primary is easily computed because of its linear proportionality to the particle density.

If we obtain inclination angle by delay times, we can use the shape of the ground distribution together with the particle density to obtain the energy and composition of the primary. This should be possible because the shape of the lateral distribution of charged particles depends differently on the composition and on the energy of the primary.

As an alternative I think it's possible to obtain a reconstruction program, which uses the ground distribution to obtain the primary energy/composition at least in the

case of vertical showers. Even if other treatments are needed to determine the inclination angle, it's probably also possible to do it in the case of inclined showers.

A program of that kind could be used at least to test the viability of the results of the simulations and determine the uncertainty. If one code is used to go one way and the same (properly modified) code is used in the inverse way it should return the original input parameters within some error.

If the inclination angle can not be determined, this alternative approach cannot be done. It’s impossible to start to propagate (or un-propagate) particles if we don’t know the direction of propagation.

6.3 Future advises

This was a very small Project and time was scarce to complete the analysis needed.

To finish this part of the analysis, and to be able to construct a program that uses the ground distribution of particles for the NAHSA project is advisable to:

- -Use the new version of CORSIKA that allows obtaining the number of particles that pass through a horizontal layer, like the AIRES. This is not really needed because for the analysis of the longitudinal development, it's only for consistency of the results of the simulation and it's not used for the final purpose of finding the energy of the primary particle given the particle density at ground level.
- -In AIRES, results should be obtained from the program that projects the density of particles, as is mentioned in the AIRES manual and use it to obtain a 2D plot of the lateral distribution.
- -Fit the AGASA function to the results obtained while changing the function parameters.
- -Use CORSIKA to obtain a similar analyses of the lateral distribution as was done for AIRES and compare the results
- -See if the AGASA function describe the CORSIKA results
- -Use other hadronic interaction models to compare the various models.
- -Calculate arrival times to be able to obtain the inclination angle of a shower.

Figures

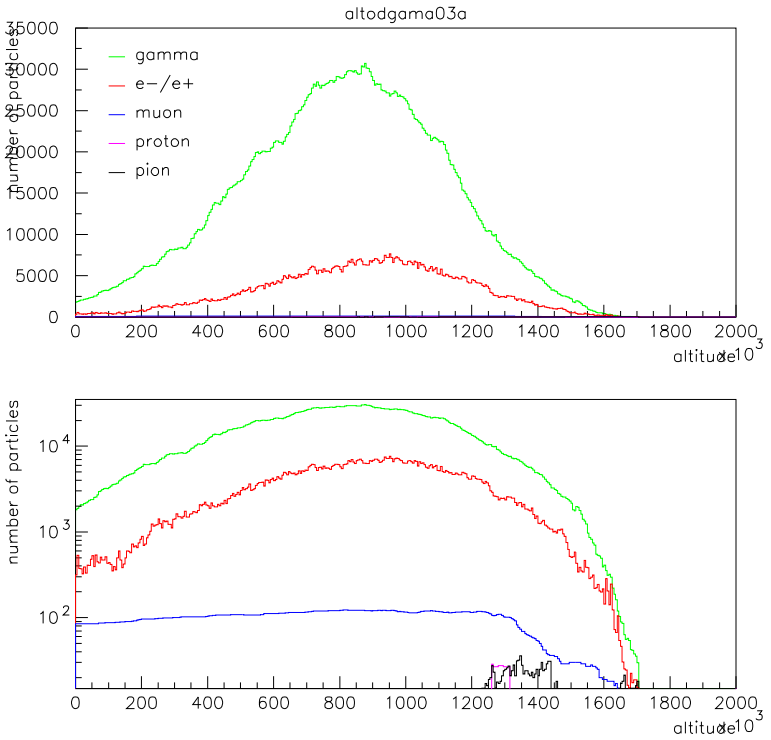

Figure 1 Longitudinal distribution - proton $E_0 = 10^{13}$ eV

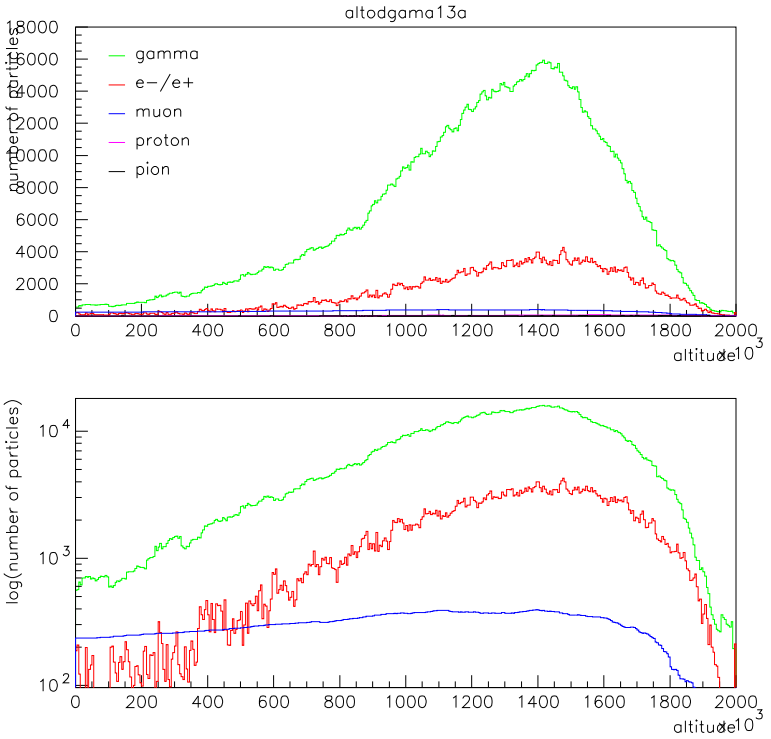

Figure 2 Longitudinal distribution - iron $E_0 = 10^{13}$ eV

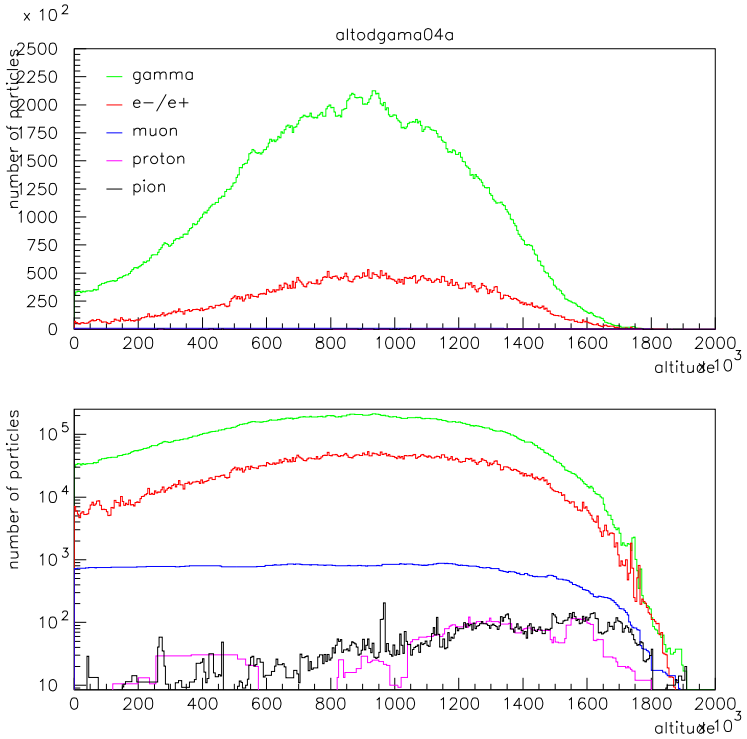

Figure 3 Longitudinal distribution - proton $E_0 = 10^{14}$ eV

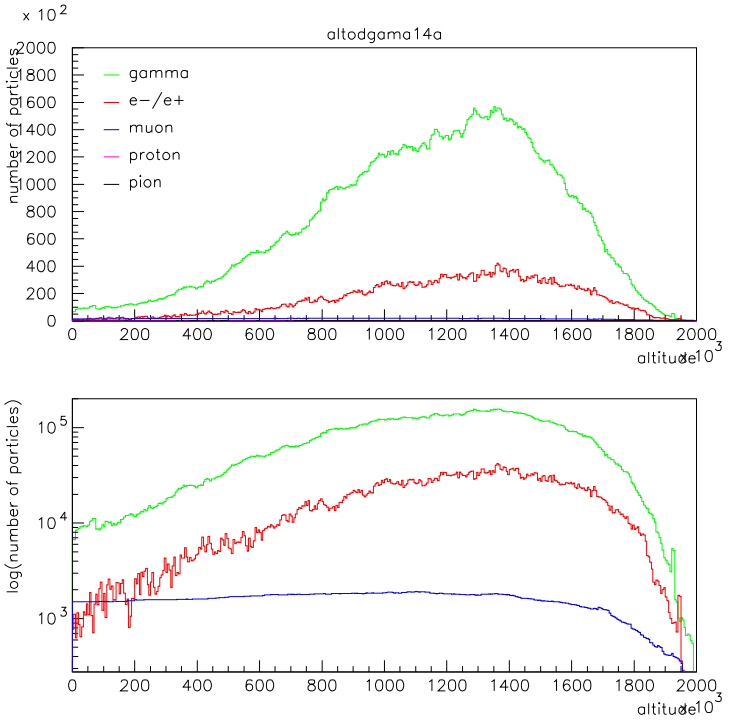

Figure 4 Longitudinal distribution - iron $E_0 = 10^{14}$ eV

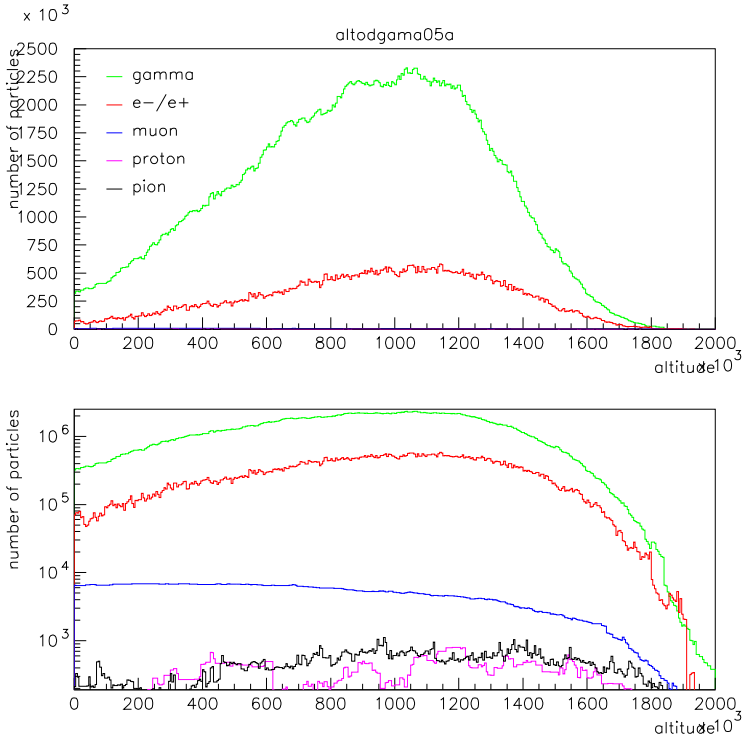

Figure 5 Longitudinal distribution - proton $E_0 = 10^{15}$ eV

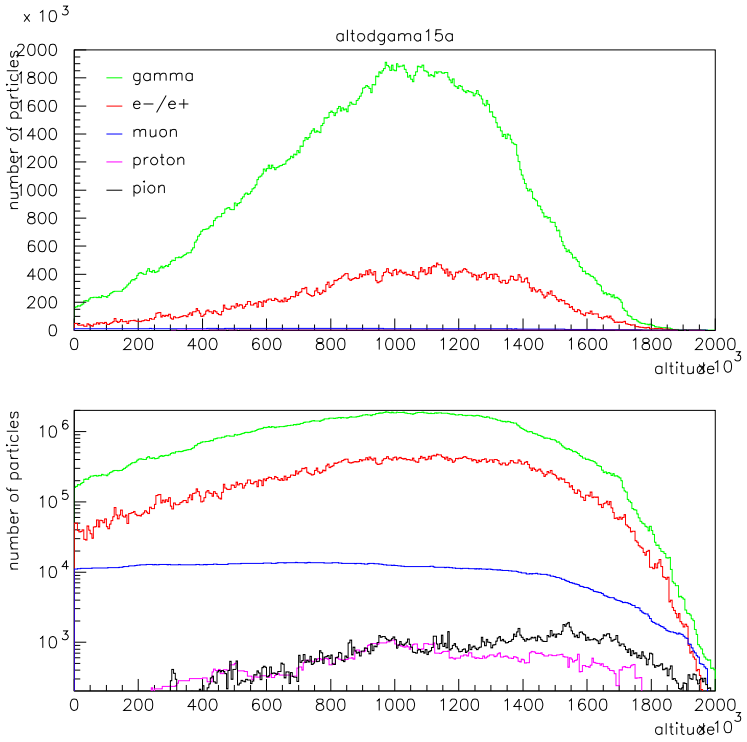

Figure 6 Longitudinal distribution - iron $E_0 = 10^{15}$ eV

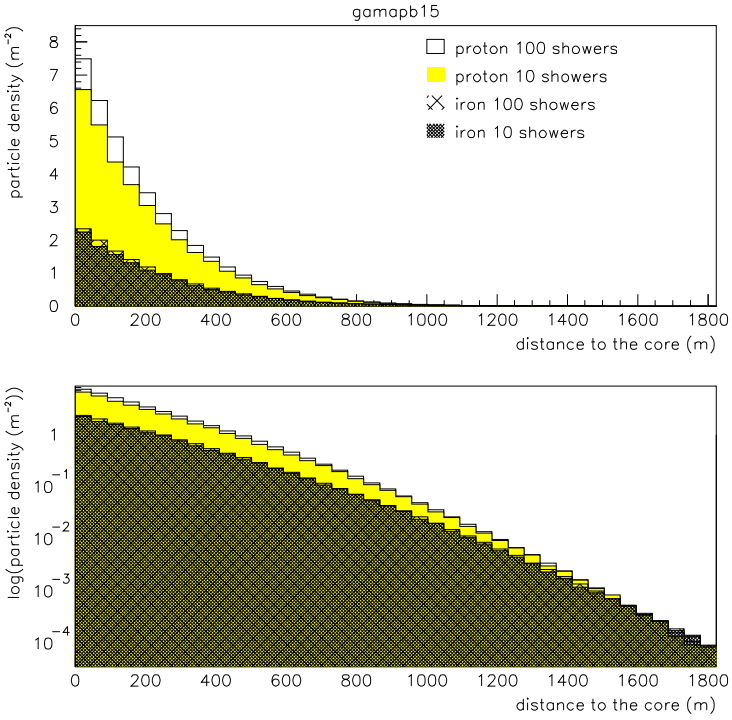

Figure 7 Gamma lateral distribution - $E_0 = 10^{15}$ eV

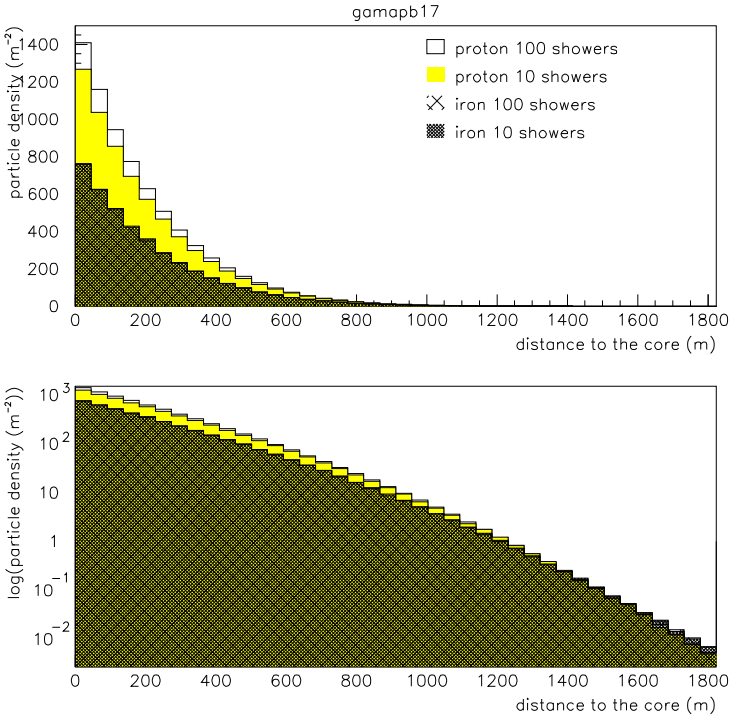

Figure 8 Gamma lateral distribution - $E_0 = 10^{17}$ eV

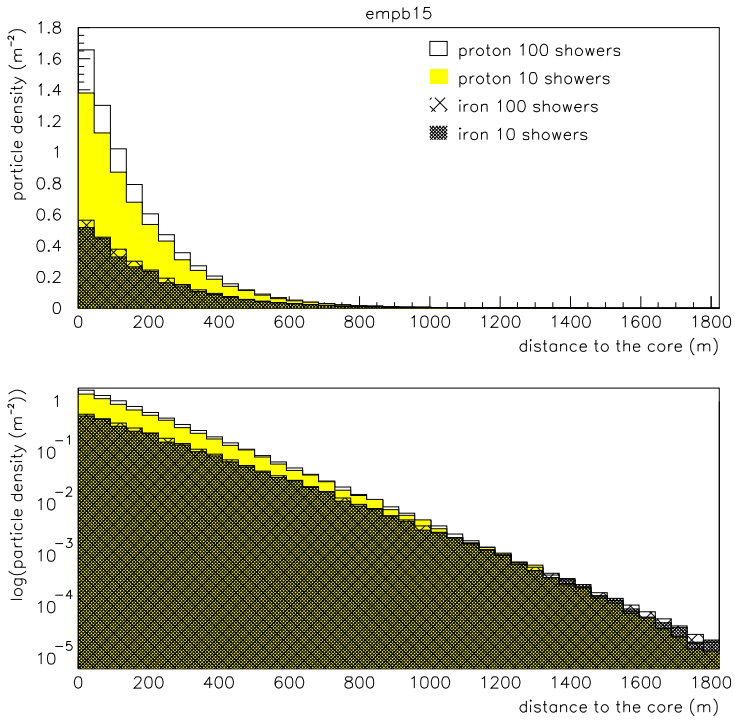

Figure 9 e^+/e^- lateral distribution - $E_0 = 10^{15}$ eV

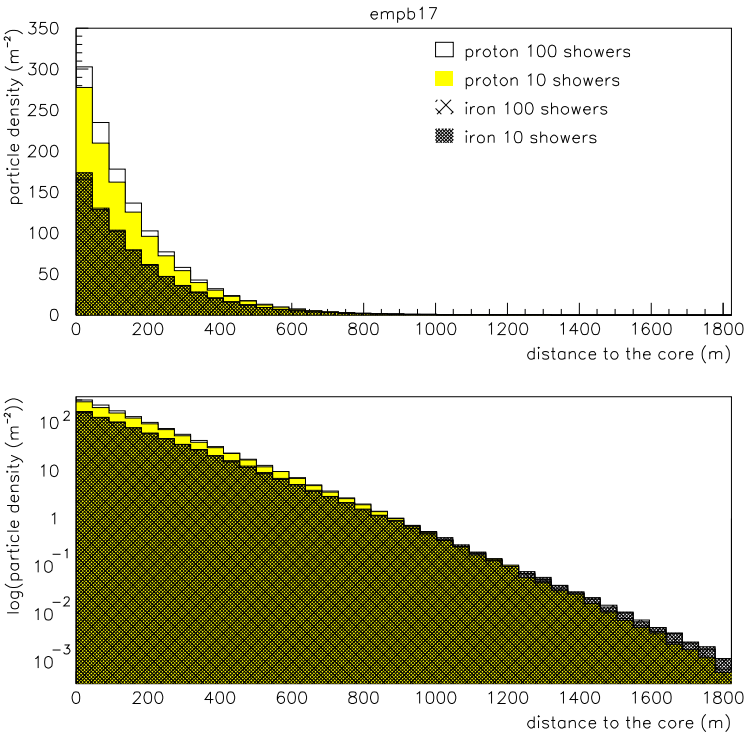

Figure 10 e^+/e^- lateral distribution - $E_0 = 10^{17}$ eV

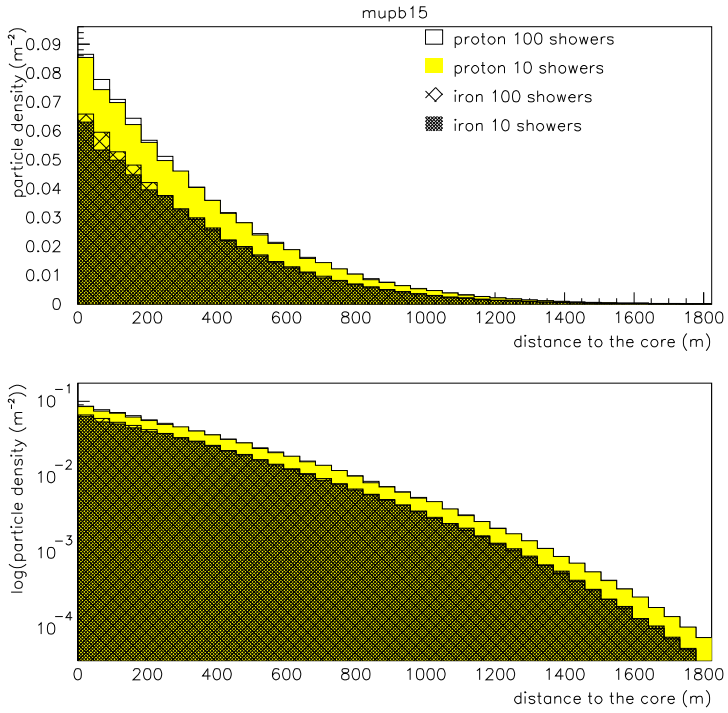

Figure 11 Muon lateral distribution - $E_0 = 10^{15}$ eV

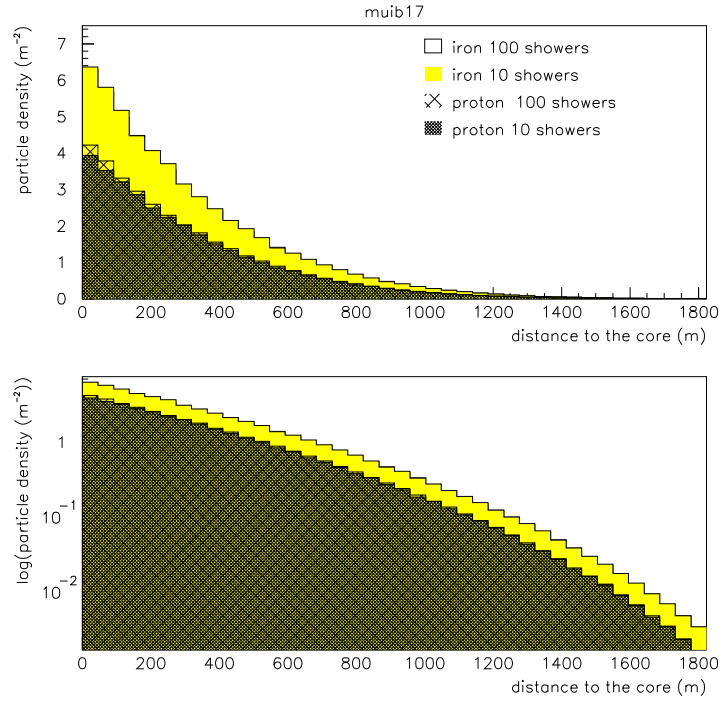

Figure 12 Muon lateral distribution - $E_0 = 10^{17}$ eV

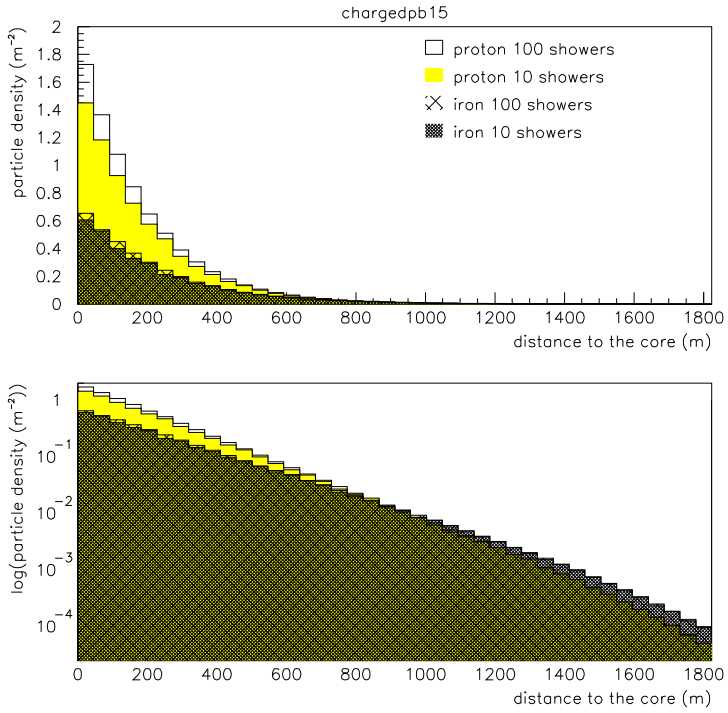

Figure 13 Charged lateral distribution - $E_0 = 10^{15}$ eV

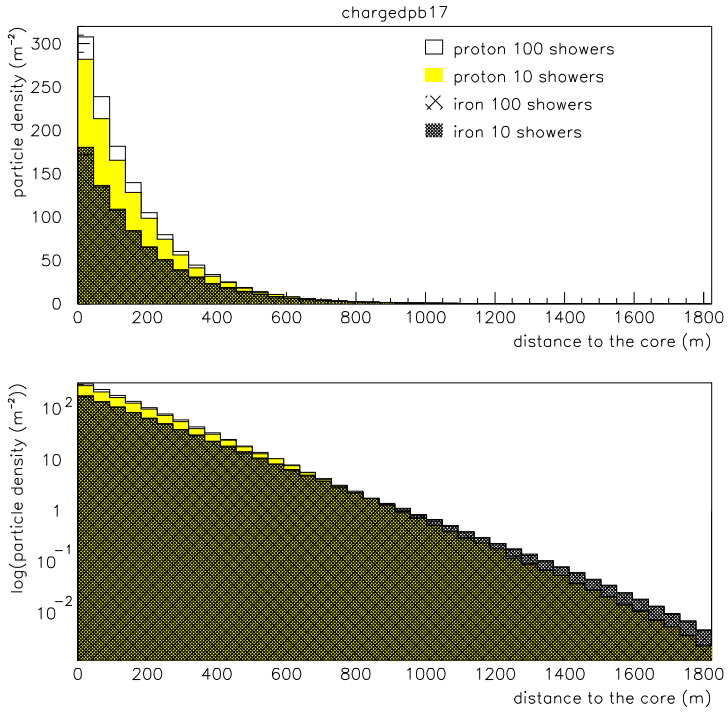

Figure 14 Charged lateral distribution - $E_0 = 10^{17}$ eV

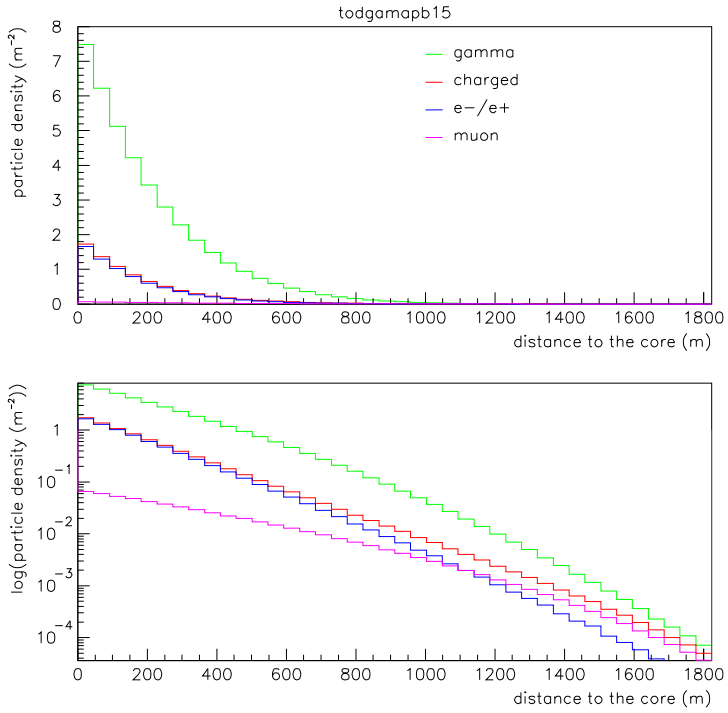

Figure 15 Lateral distribution all particles - proton with $E_0 = 10^{15}$ eV

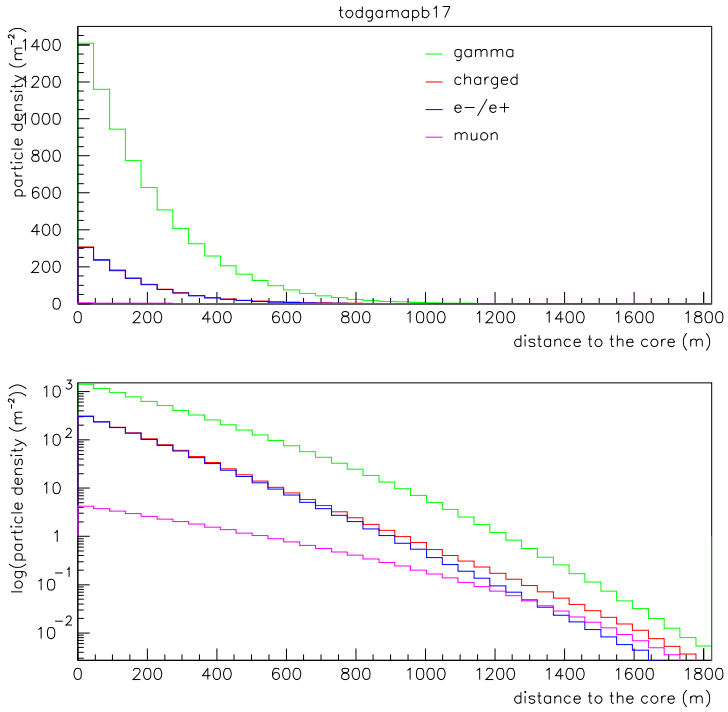

Figure 16 Lateral distribution all particles - proton with $E_0 = 10^{17}$ eV

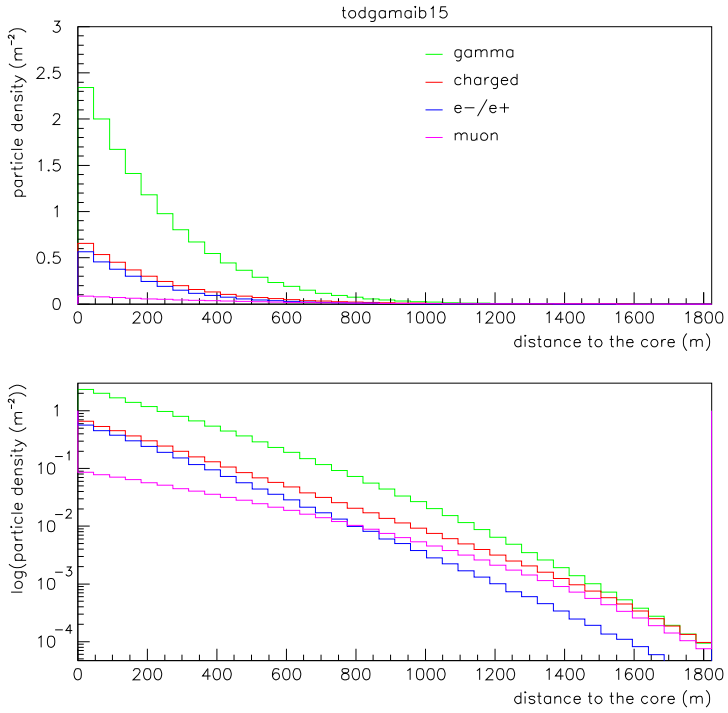

Figure 17 Lateral distribution all particles - iron with $E_0 = 10^{15}$ eV

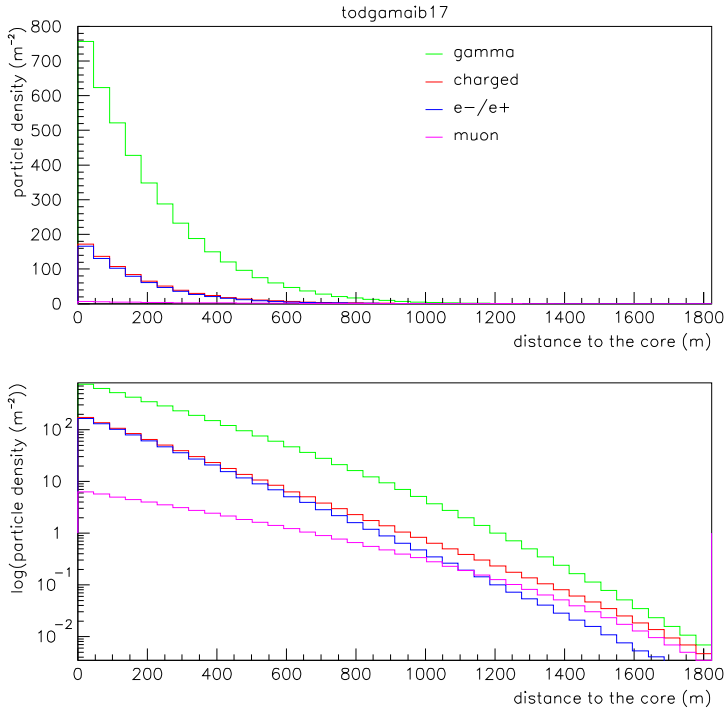

Figure 18 Lateral distribution all particles - iron with $E_0 = 10^{17}$ eV

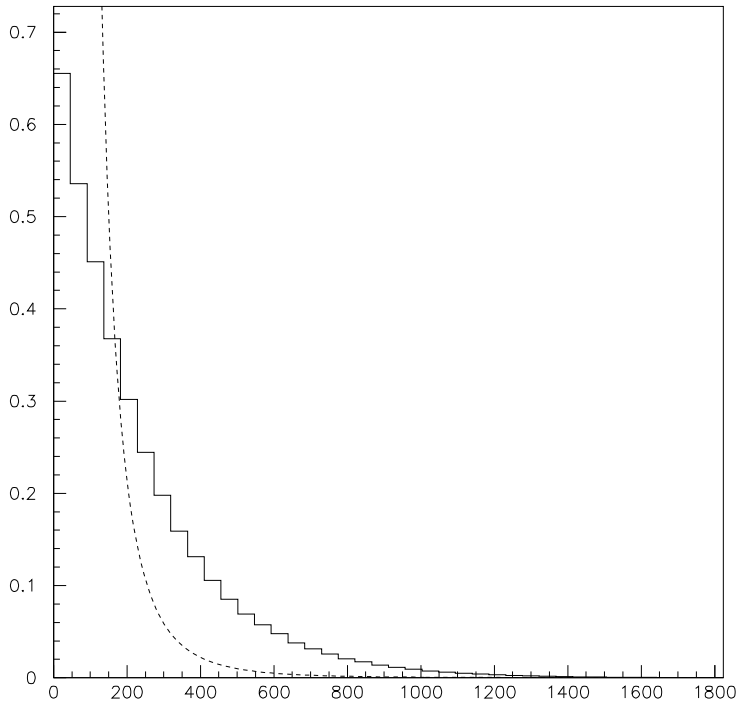

Figure 19 Charged lateral distribution - iron with $E_0 = 10^{15}$ eV with AGASA function

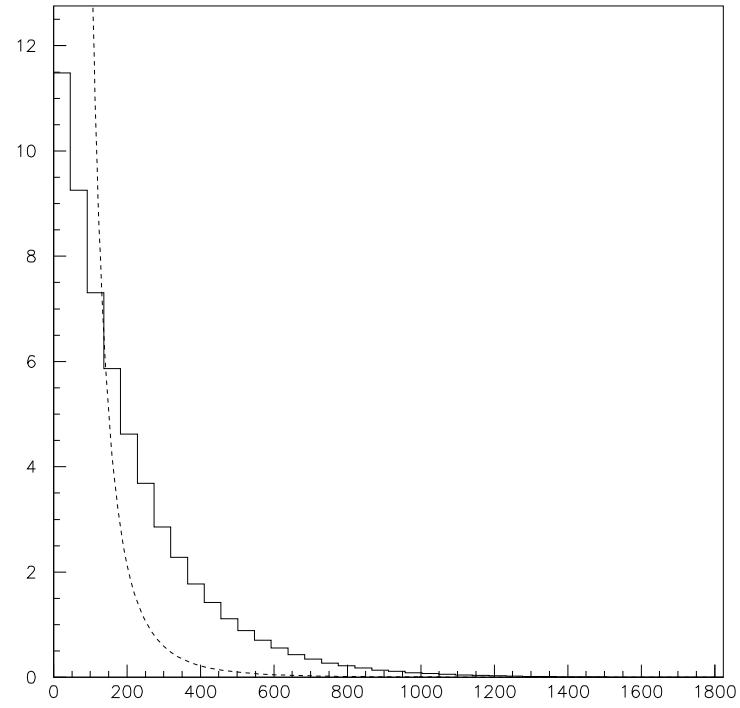

Figure 20 Charged lateral distribution - iron with $E_0 = 10^{16}$ eV with AGASA function

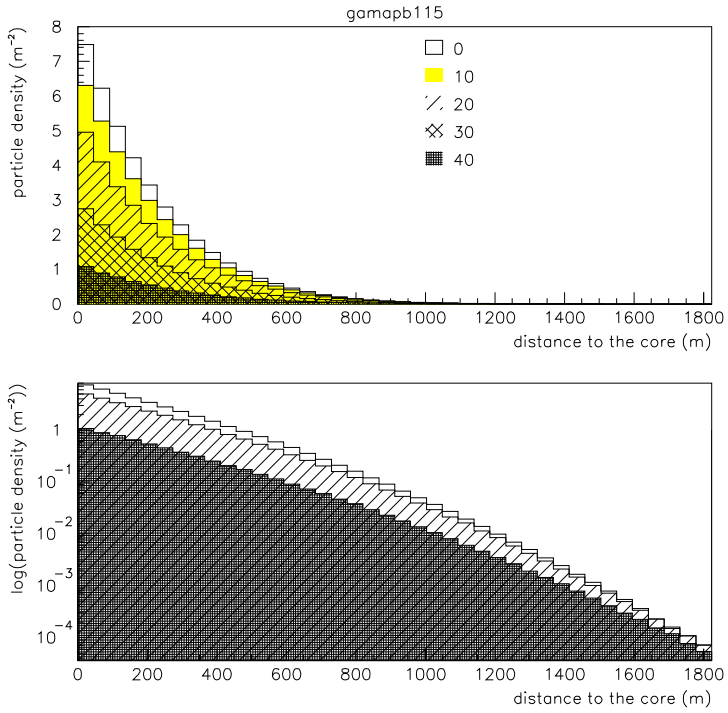

Figure 21 Gamma lateral distribution several inclinations - proton with $E_0 = 10^{15}$ eV

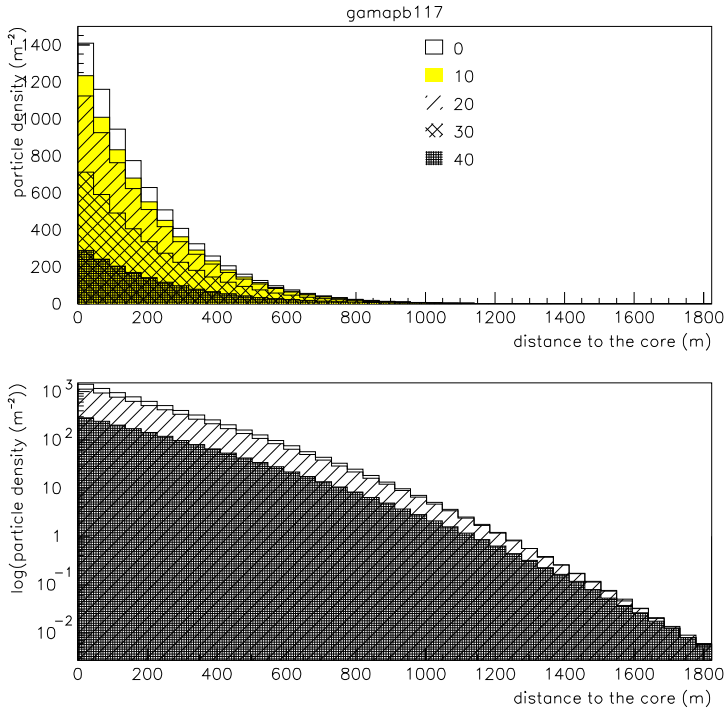

Figure 22 Gamma lateral distribution several inclinations - proton with $E_0 = 10^{17}$ eV

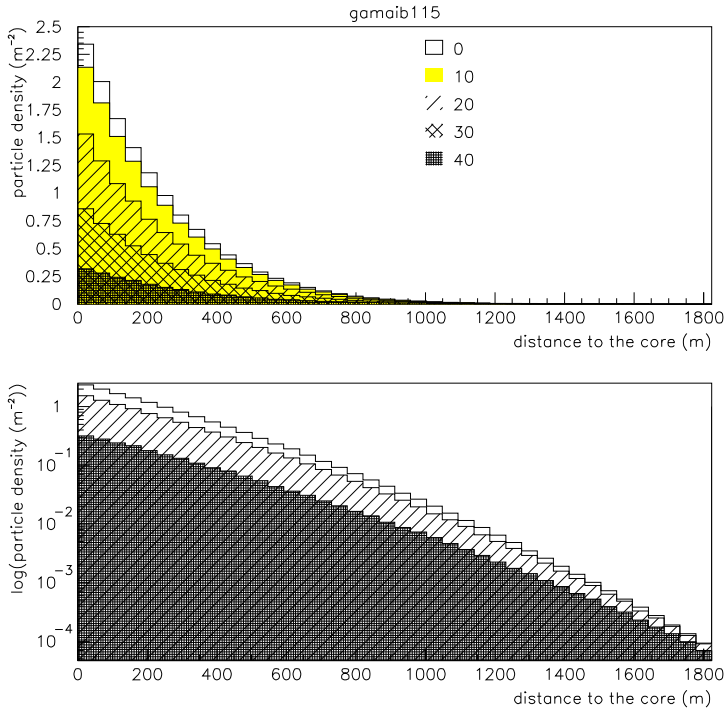

Figure 23 Gamma lateral distribution several inclinations - iron with $E_0 = 10^{15}$ eV

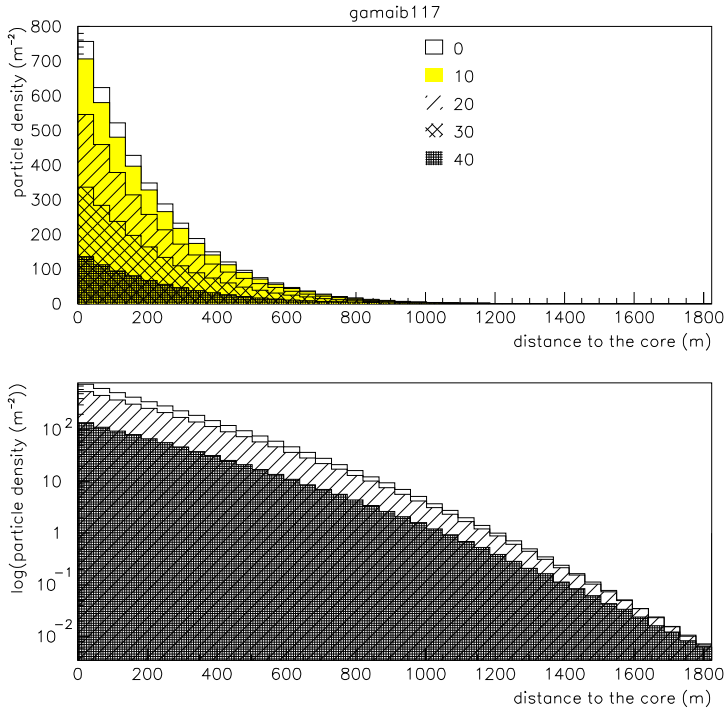

Figure 24 Gamma lateral distribution several inclinations - iron with $E_0 = 10^{17}$ eV

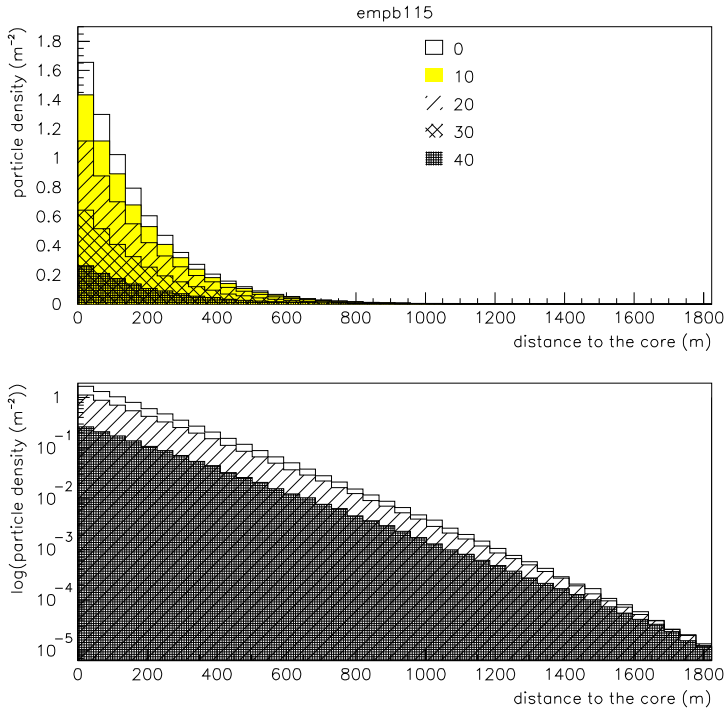

Figure 25 e^+/e^- lateral distribution several inclinations - proton with $E_0 = 10^{15}$ eV

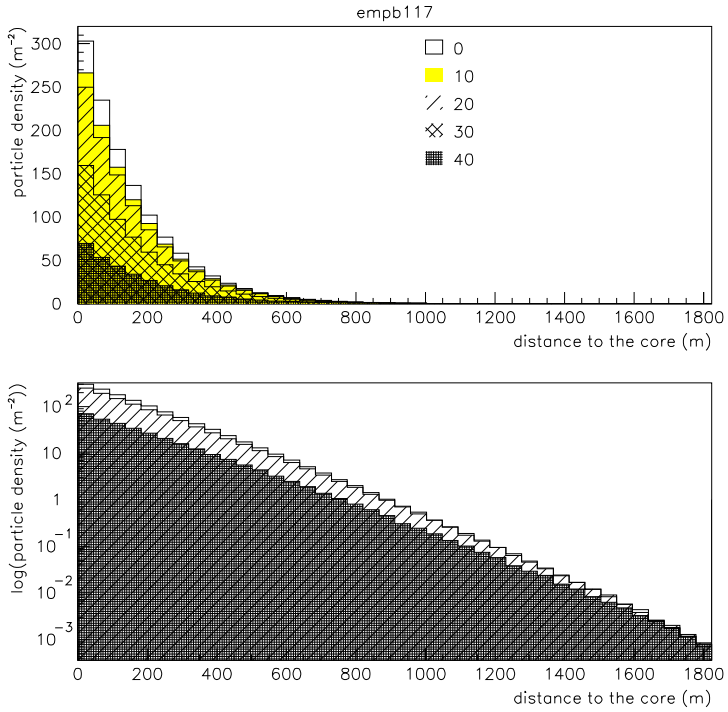

Figure 26 e^+/e^- lateral distribution several inclinations - proton with $E_0 = 10^{17}$ eV

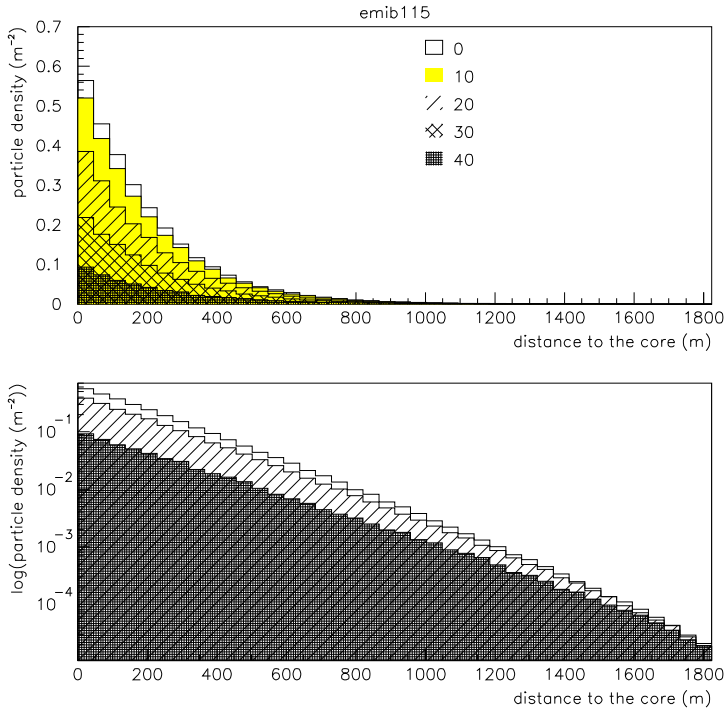

Figure 27 e^+/e^- lateral distribution several inclinations - iron with $E_0 = 10^{15}$ eV

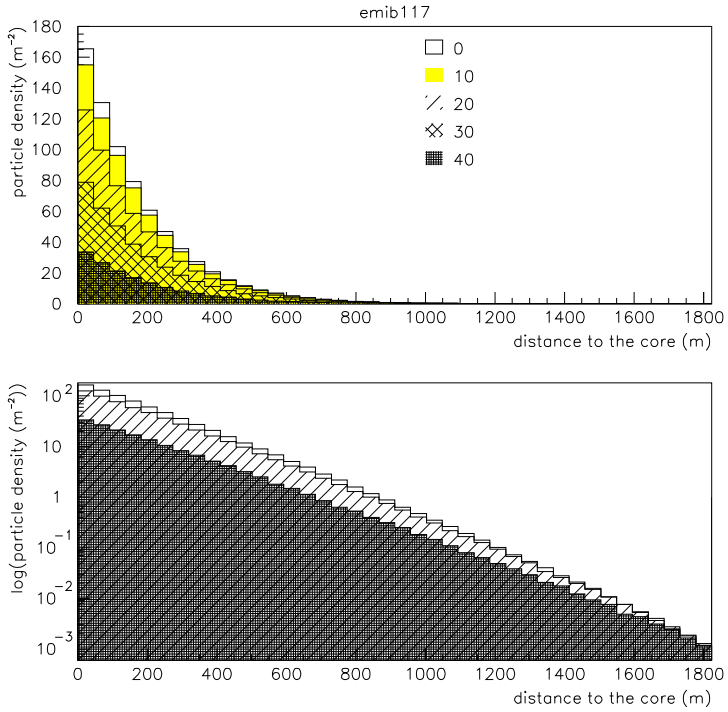

Figure 28 e^+/e^- lateral distribution several inclinations - iron with $E_0 = 10^{17}$ eV

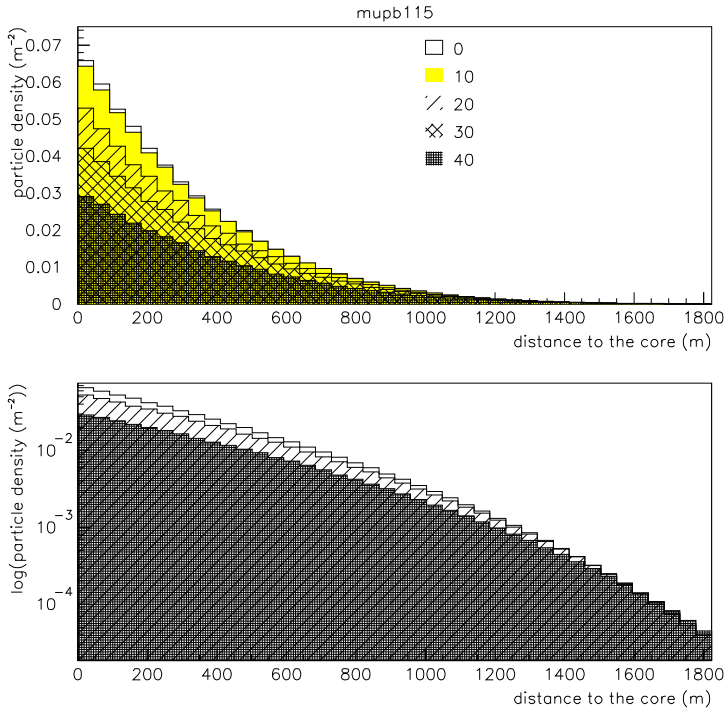

Figure 29 Muon lateral distribution several inclinations - proton with $E_0 = 10^{15}$ eV

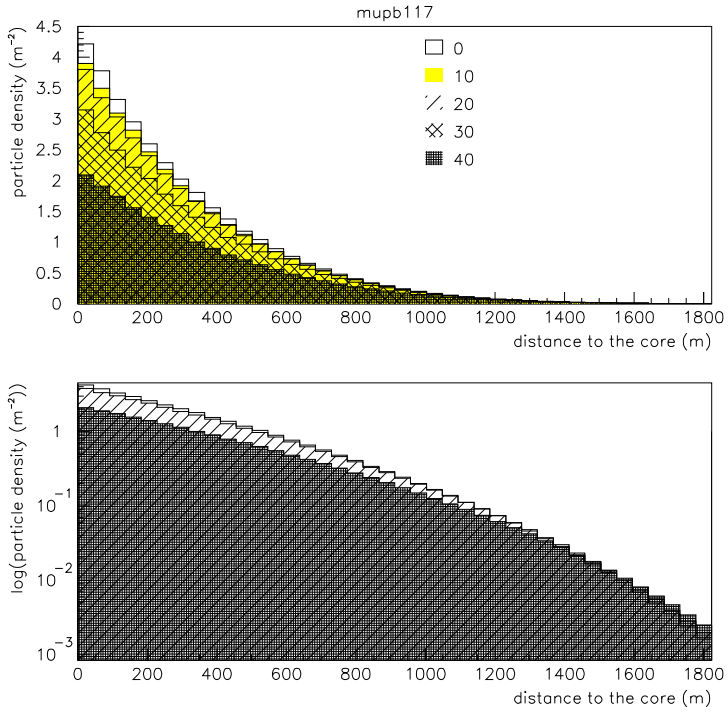

Figure 30 Muon lateral distribution several inclinations - proton with $E_0 = 10^{17}$ eV

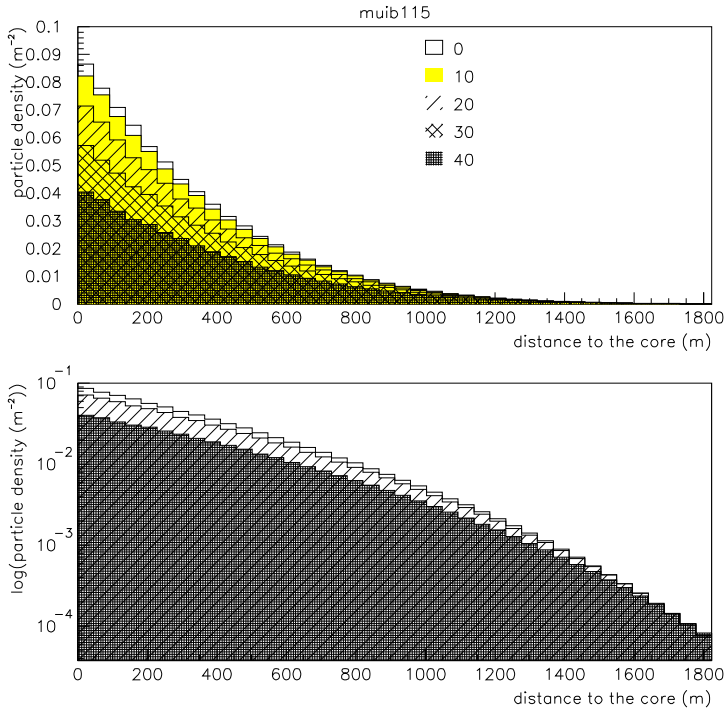

Figure 31 Muon lateral distribution several inclinations - iron with $E_0 = 10^{15}$ eV

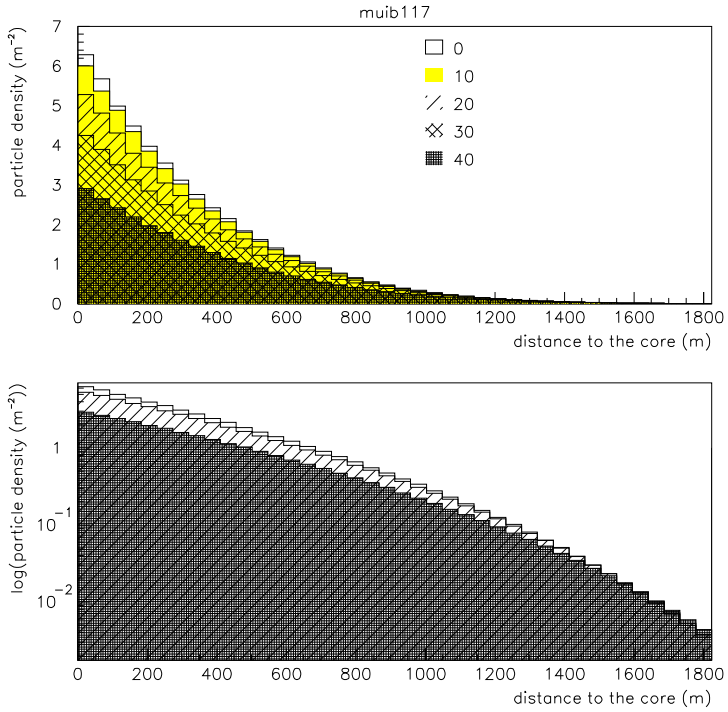

Figure 32 Muon lateral distribution several inclinations - iron with $E_0 = 10^{17}$ eV

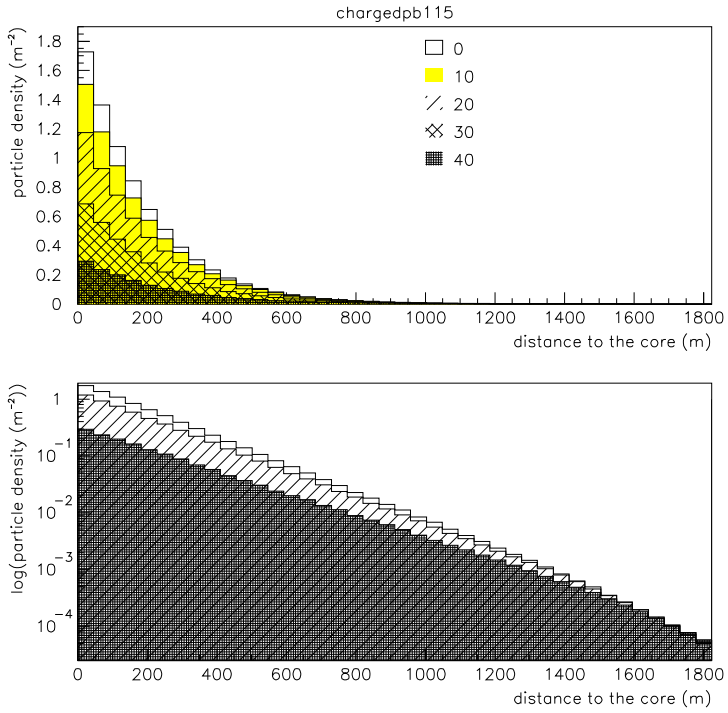

Figure 33 Charged lateral distribution several inclinations- proton with $E_0 = 10^{15}$ eV

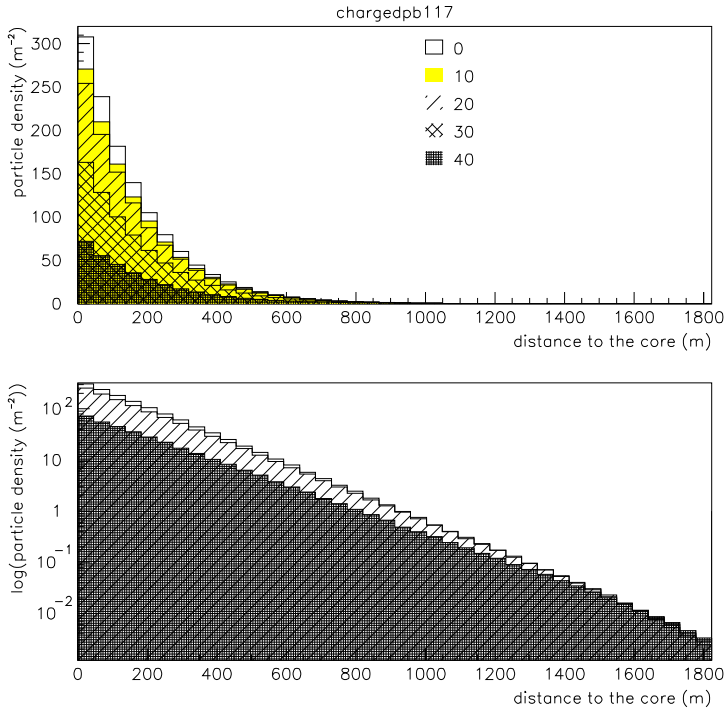

Figure 34 Charged lateral distribution several inclinations - proton with $E_0 = 10^{17}$eV

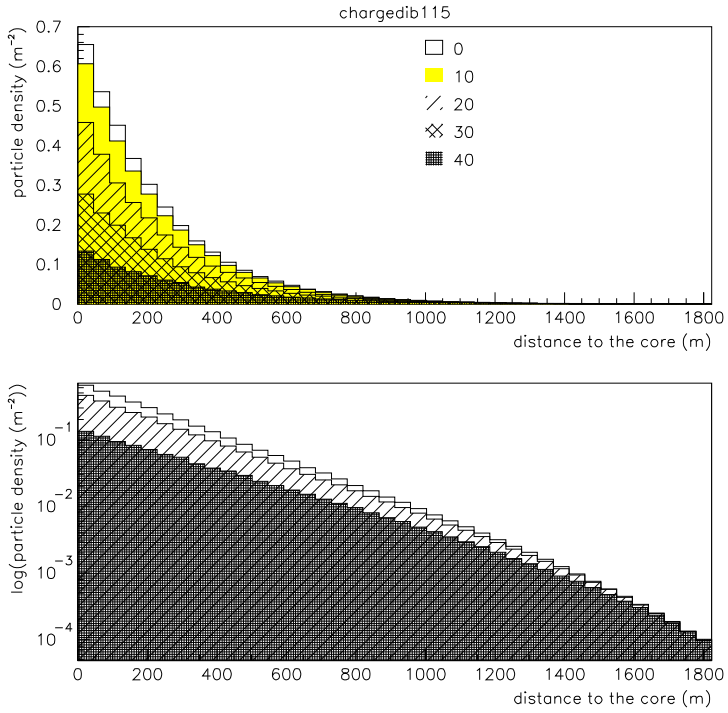

Figure 35 Charged lateral distribution several inclinations - iron with $E_0 = 10^{15}$ eV

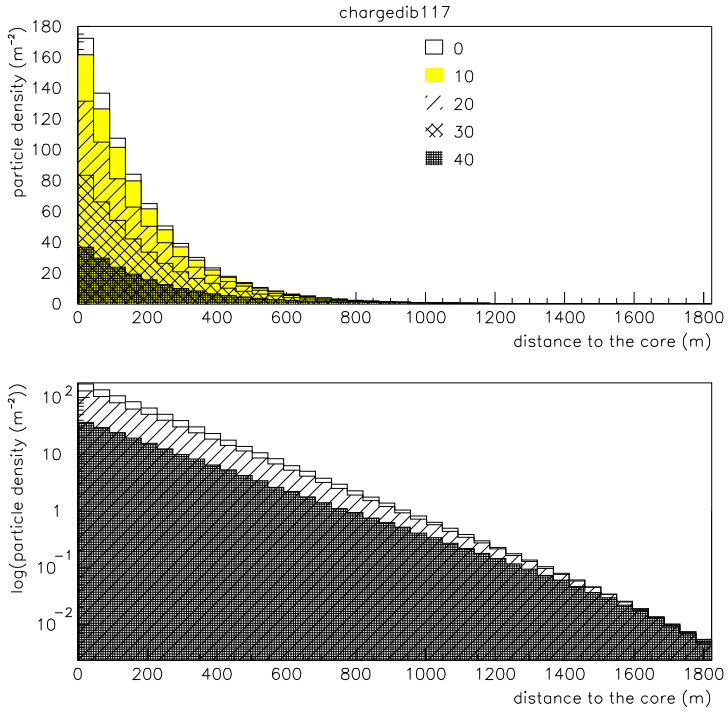

Figure 36 Charged lateral distribution several inclinations - iron with $E_0 = 10^{17}$ eV

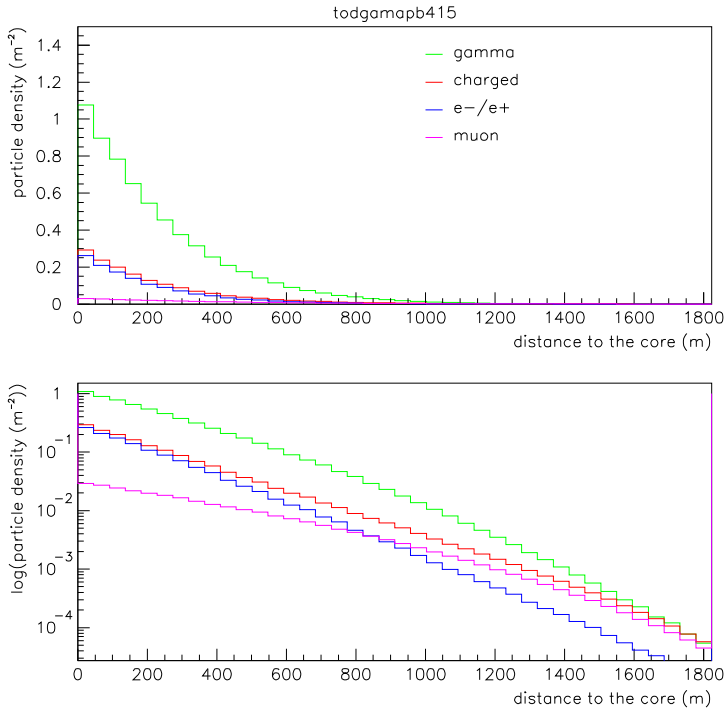

Figure 37 Lateral distribution, all particles- I = 40º, proton with $E_0 = 10^{15}$ eV

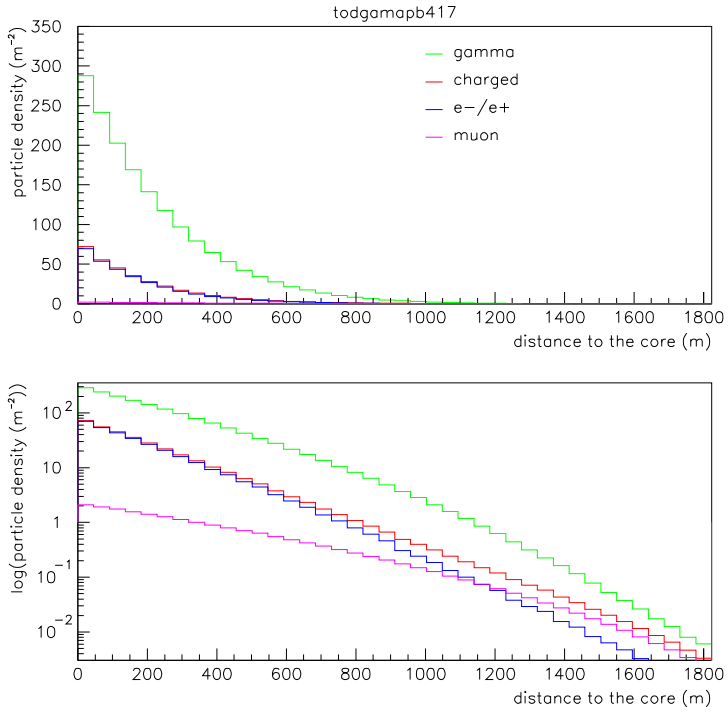

Figure 38 Lateral distribution, all particles - I = 40º, proton with $E_0 = 10^{17}$eV

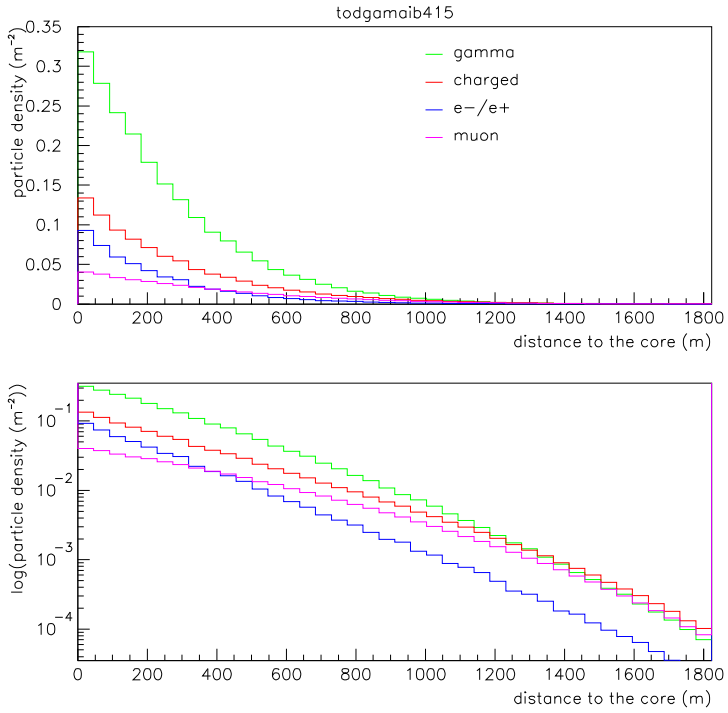

Figure 39 Lateral distribution, all particles - I = 40º, iron with $E_0 = 10^{15}$ eV

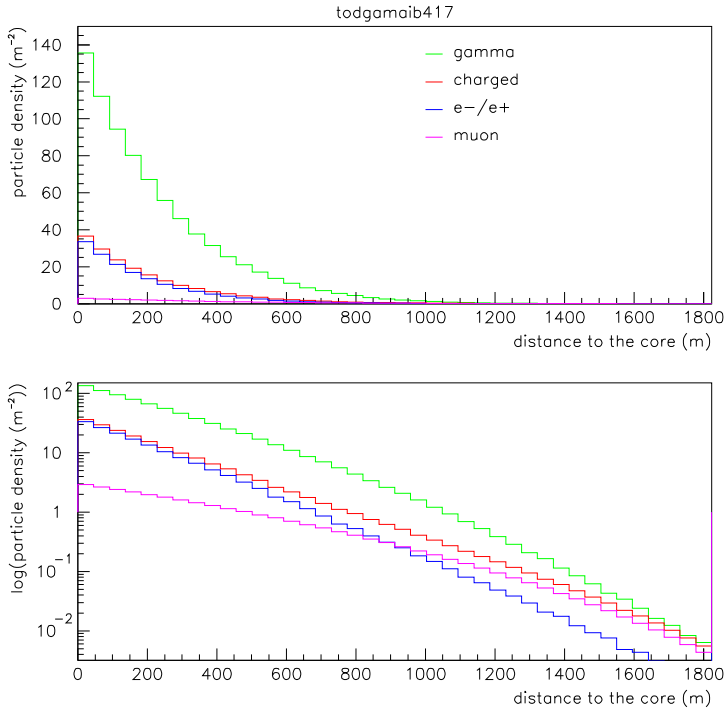

Figure 40 Lateral distribution, all particles – I = 40º, iron with $E_0 = 10^{17}$ eV

Appendix A

A.1 CORSIKA Typical Input File

```
RUNNR   4                       number of run
EVTNR   1                       number of first shower event
NSHOW   1                       number of showers to generate
PRMPAR  14                      particle type of prim. particle
ESLOPE  -2.7                    slope of primary energy spectrum
ERANGE  1.E5 1.E5               energy range of primary particle (GeV)
THIN    1.E-16 1                thinnig options
THETAP  0.  0.                  range of zenith angle (degree)
PHIP    0.  360.                range of azimuth angle (degree)
SEED    725   0   0             seed for 1. random number sequence
SEED    527   0   0             seed for 2. random number sequence
SEED    429   0   0             seed for 3. random number sequence
OBSLEV  0.                      observation level (in cm)
ATMOD   5                       Atmospheric Model
ELMFLG  T   T                   em. interaction flags (NKG,EGS)
RADNKG  200.E2                  outer radius for NKG lat.dens.determ.
ARRANG  0.                      rotation of array to north
FIXHEI  0.  0                   first interaction height & target
FIXCHI  0.                      starting altitude (g/cm**2)
MAGNET  20.0  42.8              magnetic field centr. europe
HADFLG  0  0  0  0  0  0        flags for hadr. Interaction hadrons
SIBYLL  T 0                     use venus for high energy hadrons
SIBSIG  T                       use VENUS hadronic cross sections
ECUTS   0.3 0.3 0.003 0.003     energy cuts for particles
MUADDI  F                       additional info for muons
MUMULT  T                       muon multiple scattering angle
MAXPRT  10                      max. number of printed events
ECTMAP  1.E4                    cut on gamma factor for printout
STEPFC  10.                     mult. scattering step length fact.
DEBUG   F  8  F  1000000        debug flag and log.unit for out
PLOTSH T                        option to create the particle files
DIRECT  ../results/             output directory
EXIT                            terminates input
```

A.2 AIRES Typical Input File

```
Task                proton03
Primary             proton
PrimaryEnergy       10  TeV
TotalShowers        1
PrimaryZenAngle     0 deg
GroundAltitude      45  m
ObservingLevels     400
Thinning            1.e-4 Relative

GammaCutEnergy      3.0 MeV
ElectronCutEnergy   3.0 MeV
MuonCutEnergy       1.0 GeV
NuclCutEnergy       300.0 MeV

AddSite             Nijmegen 51.8333 deg 5.8667 deg 45 m
Site                Nijmegen
Date                2002 10 10

ADF                 On     # Save the ASCII version of IDF file after
                           #finishing the simatutions

ExportTables        1205 Opt s       #      Longit devel of e+ e e-
ExportTables        1207 Opt s       #      Longit devel of mu+ e mu-
ExportTables        1022 Opt s       #      Longit devel of proton
ExportTables        1001 Opt s       #      Longit devel of gamma
ExportTables        1211 Opt s       #      Longit devel of pion

End
```

Appendix B

B.1 Count the number of particles in CORSIKA

```
#include<stdio.h>

FILE *fp;

main(argc,argv)
     int argc;
     char **argv;
{
  int n_read,i,j;
  float k;
  float part[8],tmp[1],number[400], count[400];

  if((fp = fopen(argv[1],"r")) == NULL){
    printf("The file %s cannot be opened\n",argv[1]);
    exit(0);
  }

  for(j=0;j<400;j++) count[j] = 0.;

  number[0]=0;
    for(j=1;j<400;j++) number[j] = number[j-1]+5000;

 n_read = fread(tmp,4,1,fp);
  while(n_read > 0){
    n_read = fread(part,4,8,fp);

    k=0;
    for(j=0;j<400;j++) {
      if(
          ((k<part[4]) && (k+5000>part[4]) )  ||
          ((k<part[7]) && (k+5000>part[7]) ) ||
          ((k>=part[7]) && (k+5000<=part[4]) ))  {
      if((part[0] == 5) || (part[0] == 6)){
        if(part[1] >=1.) count[j]++;
      }else{
         count[j]++;
      }
      }
      k=k+5000;
    }
    n_read = fread(tmp,4,1,fp);
    n_read = fread(tmp,4,1,fp);

  }
  fclose(fp);

  for(i=0;i<400;i++) {
  printf("%13g ",number[i]);
  printf("%13g ",count[i]);
  printf("\n");
  }
}
```

B.2 transforming atmospheric depth in altitude in AIRES

```
#include<stdio.h>
#include<math.h>

FILE *fp;

char buf[500];
main(argc,argv)
     int argc;
     char **argv;
{
  int n_read,i;
  float part[7],a[5],b[5],c[5],xl[6],tmp[1],x ;

  a[0]=-186.5562;
  a[1]=-94.91;
  a[2]=0.61289;
  a[3]=0.0;
  a[4]=0.01128292;

  b[0]=1222.6562;
  b[1]=1144.9069;
  b[2]=1305.5948;
  b[3]=540.1778;
  b[4]=1.0;

  c[0]=9941.8638;
  c[1]=8781.5355;
  c[2]=6361.4304;
  c[3]=7721.7016;
  c[4]=1.0e7;

  xl[0]=1036.1;
  xl[1]=631.0998;
  xl[2]=271.7;
  xl[3]=3.0395;
  xl[4]=0.0012829;

  if((fp = fopen(argv[1],"r")) == NULL){
    printf("The file %s cannot be opened\n",argv[1]);
    exit(0);
  }

  while(fgets(buf,499,fp) == buf){
    if(buf[0] == '#') continue;
    //    printf("-->%s",buf);

    if(sscanf(buf,"%g %g %g %g %g %g %g",&part[0],&part[1],
        &part[2],&part[3],&part[4],&part[5],&part[6]) != 7) continue;
    x=part[1];

     if((x<=xl[4]) && (x>0)) {
           part[1]=(c[4]*(a[4]-x))/b[4];
            }else{
            for (i=0;i<4;i++){
```

```
            if((x>xl[i+1]) && (x<=xl[i])){
            part[1]=-c[i]*log((x-a[i])/b[i]);
          }
          }
        }

  for(i=1;i<3;i++) printf("%13g ",part[i]);
  printf("\n");
}

fclose(fp);
}
```

B.3 AGASA Function and Plot Routine

AGASA Function

```
      function agasa2(x)

      Vector Energy
      alp = 1.2
      rm = 91.60
      rn = 3.84
      rkm = 1000.
      delta = 0.6
      R = 600.
      area = 100*100
      agasa = (R/rm)**(-1.*alp)
      agasa = agasa*(1.+R/rm)**(-1.*(rn-alp))
      agasa = agasa*(1.+(R/rkm)**2)**(-1.*delta)
      ag600 = area*(Energy(1)/(2.0E8*agasa*1.E4))
      R = abs(x)
      agasa = ag600*(R/rm)**(-1.*alp)
      agasa = agasa*(1.+R/rm)**(-1.*(rn-alp))
      agasa2 = agasa*(1.+(R/rkm)**2)**(-1.*delta)
      return
      end
```

Paw kumac to overplot the AGASA function and the lateral charge distribution

```
opt zfl
v/read height,npar [1]
v/inp energy(1)   [2]
h/cre/1d 10 ' ' 40 0. 1823.81
put/cont 10 npar
h/pl 10
h/cre/title [1]
h/atitle 'distance to the core (m), particle density (m^-2) '
v/cre energy r [2]
fun/pl agasa2.f 0. 1823.81 s
p/print [1].eps
```

References

Anchordoqui, L. A.; Sciutto, S. J.; Dova, M. T.; *Extensive Air Showers rounded up by AIRES + SIBYLL/QGSJET,* astro-ph 9905248 (1999)

Erwin, George; *The NAHSA Project*, Master Thesis, Nijmegen University, (2002)

Gaisser, T. K.; *Cosmic Rays and Particle Physics*, Cambridge University Press (1990)

Griffiths, David; Introduction to Elementary Particles, John Wiley & Sons (1987)

Heck, D. et al.; *CORSIKA: A Monte Carlo Code to Simulate Extensive Air Showers*, Forschungszentrum Karlsruhe, FZKA 6019 (1998).

Knapp, J.; Heck, D.; *Extensive Air Showers Simulations with CORSIKA: User's Guide* (Version 6.016), Forschungszentrum Karlsruhe, (2002).

Knapp, J.; Heck, D.; Sciutto, S. J.; Dova, M. T.; Risse, M.; *Extensive Air Showers Simulations at Highest Energies,* astro-ph 0206414 (2002)

Nagano, M.; Watson, A. A.; *Observations and Implications of Ultrahigh-energy Cosmic Rays*, Rev. Mod. Phys. 72,3 686 (2000)

Sciutto, S. J.; The AIRES System for Air Shower Simulations. An Update, ICRC (2001)

Sciutto, S. J.; AIRES: *A system for air shower simulations User's guide and reference manual* (Version 2.6.0), Departamento de F´ýsica Universidad Nacional de La Plata (2002)

The NAHSA-website: http://www.hef.kun.nl/nahsa